Supplementary Data for

Template-assisted synthesis of adenine-mutagenized cDNA by a retroelement protein complex

Sumit Handa[1], Yong Jiang[2], Sijia Tao[2], Robert Foreman[1], Raymond F. Schinazi[2], Jeff F. Miller[3], and Partho Ghosh[1,*]

[1]Department of Chemistry & Biochemistry, University of California, San Diego, CA 92093, USA.
[2]Center for AIDS Research, Laboratory of Biochemical Pharmacology, Department of Pediatrics, Emory University School of Medicine, Atlanta, GA 30322, USA.
[3]Departments of Microbiology, Immunology, and Molecular Genetics, Molecular Biology Institute, and California NanoSystems Institute, University of California, Los Angeles, Los Angeles, CA 90095, USA.

Contents:

Supplementary Material and Methods

Cloning, Expression, and Purification of Proteins. The coding sequence of *Bordetella* bacteriophage bRT was amplified by PCR and inserted between the BamHI and HindIII restriction sites of a modified pET-28b (Novagen) expression vector. The coding sequence of *Bordetella* bacteriophage Avd was amplified by PCR and inserted between the NdeI and XhoI restriction sites of pACYCDuet-1 vector (Novagen). The integrity of the bRT and Avd coding sequences was confirmed by DNA sequencing. The two plasmids were co-transformed into *Escherichia coli* BL21-Gold (DE3). Transformed bacteria were grown in LB media with 50 µg/mL kanamycin and 20 µg/mL chloramphenicol. Centrifugation to harvest the bacteria was carried out for 30 min at 3,000 x *g* at 4 °C.

Twenty mL of buffer A (500 mM $(NH_4)_2SO_4$, 50 mM HEPES, pH 8.0, 0.1% β-mercaptoethanol, 20% glycerol) per L of bacterial culture was used for resuspension of bacteria. Bacterial lysis using the Emulsiflex C-5 was carried out at 1,000 bar for 3 cycles, and centrifugation of the lysate and the lysate was centrifuged for 30 min at 35,000 x *g* at 4 °C. All subsequent purification steps were performed at 4 °C. The supernatant was applied to a column containing His-Select® Nickel affinity gel (Sigma; 1 ml of resin per 20 mL of bacterial lysate), which had been equilibrated with buffer A. The column was washed with five column volumes of buffer A containing 40 mM imidazole, and the column was then incubated with buffer A containing DNase I (0.25 units/mL) and RNase A/T1 mix (0.2 µL/mL) at room temperature for 30 min. The column was next washed with 10 column volumes of buffer A containing 40 mM imidazole. The bRT-Avd complex was eluted from the column with buffer A containing 250 mM imidazole. The His-tag was removed by adding PreScission protease (approximately 1:50 protein:protease mass ratio) to the eluate and incubating overnight at 4 °C. The bRT-Avd complex was further purified by gel filtration chromatography on a Superdex 200 column run in 300 mM $(NH_4)_2SO_4$, 20 mM HEPES, pH 8.0, 1 mM dithiothreitol (DTT), and 10% glycerol. The bRT-Avd complex was loaded onto the column directly without an exchange of buffer.

Purified bRT-Avd and bRT were concentrated through ultrafiltration (10 kDa MWCO Amicon, Millipore) to 2 mg/mL. The concentrations of bRT-Avd and bRT were

determined using a calculated molar extinction coefficient at 280 nm of 157,110 $M^{-1}cm^{-1}$ (with a 1:5 bRT:Avd stoichiometry) and 64,860 $M^{-1}cm^{-1}$, respectively.

RNA Synthesis and Purification. Linear template DNA was produced by PCR amplification and contained at its 5' end a T7 polymerase promoter sequence (TAATACGACTCACTATA) followed by GG to promote transcription. The sequence of interest immediately followed the GG. Products of the transcription reaction were filtered through a 0.22 µm filter and extracted with two volumes of phenol:chloroform:isoamyl alcohol (25:24:1 v/v). Ammonium acetate, pH 6.0 was added to the aqueous phase to a final concentration of 3 M, after which 2.5 volumes of 100% ethanol were added. The sample was incubated at -80 °C for 30 min and then precipitated by centrifugation (30 min, 16,000 x *g*, 4 °C). The concentration of RNA samples was determined by absorption at 260 nm (A_{260}), and the purity of the samples determined by the A_{260}:A_{280} ratio.

Quantification of dNTPs in *Bordetella*. *Bordetella* was harvested by centrifugation for 30 min at 16,000 x *g* at 4 °C. For separation of intracellular deoxynucleotides using a Kinetex EVO C18 column (100 × 2.1 mm) with 5 µm particle size (Phenomenex, CA, USA), a flow rate of 250 µL/min was used, and solvent A (2 mM $NH_3H_2PO_4$ with 3 mM hexylamine) and solvent B (acetonitrile) were used in a gradient elution program as follows: 3% from 0 to 3 min, 3% to 17% from 3 to 11 min, 17% to 80% B from 11 to 13 min and 80% B from 13 to 15 min. The equilibration time between two injections was 10 min. Multiple reaction monitoring using an API5000 triple quadrupole mass spectrometer (ABsciex, MA, USA) was as follows: dATP (492→136), dCTP (468→112) and dGTP (508→152) in positive mode with $^{13}C^{15}N$-dATP (507→146), $^{13}C^{15}N$-dCTP (480→119) and $^{13}C^{15}N$-dGTP (523→146) as internal standards, and TTP (481→158.8) and dUTP (467→158.8) in negative mode with $^{13}C^{15}N$-TTP (493→158.8) as internal standard. The MS parameters for the analytes were set as follows: ion spray voltage, 5500 V (positive mode) or 4500 V (negative mode); curtain gas, 25 psi; ion source gas 1, 40 psi; ion source gas 2, 40 psi; source temperature, 500°C and collision gas, 10 psi. Analyst software version 1.5 was used to operate the mass spectrometer and to

perform data analysis. Calibration curves were generated from standards of dATP, dCTP, dGTP, TTP and dUTP by serial dilutions, ranging from 2.5 nM to 1000 nM for dATP, dCTP, dGTP and TTP, and 0.5 nM to 200 nM for dUTP. All calibration curves had r^2 value greater than 0.99.

Table S1. Scrambled Sp Sequences

Sp 19-34	GGTTGCGACGTCGGCG
Sp 4-8	ACTGG
Sp 9-13	ACTTC
Sp 14-18	CGCGC
Sp 35-39	ATTCG
Sp 40-44	GATCA
Sp 45-49	TCCTC

Table S2. DNA oligonucleotides

P^{avd}	CTTTGCGATTCACGCGGGCA
P^{G117}	ATGCAAGAAGGTGATGGGCA
P^{A56}	GAAGCAGGACAGAACCGGCT
Primer 5'-pET28b	GAATTCGGATCCGCGACCCA
Primer 3'-pET28b	GGCCGGAAGCTTTTTTTTTTTTTTTTTTT
Primer 1	GGCAAATCTAGACGCTGCTGCGCTATTCGGCG
Primer 2	GCCCTGAAGCTTCCCATCACCTTCTTGCATGG
Primer 3	ATAATAAAGCTTTTTTTTTTTTTTTTTTT
Primer 4	ACCCGGGGATCCCAGACGCCGCGCGCCCCG
Primer 5	ATAATAAAGCTTCAGACGCCGCGCGCCCCGAT
Primer 6	ACCCGGAAGCTTGAAGTCGGCCCCGCCTTTCCA
Primer 7	ACCCCCGGATCCCTCATT
Primer 8	GAAATTAATACGACTCACTATAGGGGCAGGCTGGGAAATAACGCT
Primer 9	GCCCTGAAGCTTGAAGTCGGCCCCGCCTTTCCA
Adapter	ACCCCCGGATCCCTCATTTCCCTTTTGCTAGAATTCGGATGGCCGACCCA
Splint-1	CCGAAGCAGGACAGAACCGGCC TATTGAGGAAAGGCCAGC
Splint-2	GCCGAAGCAGGACAGAACCG CGGCCATCCGAATTCTAGCAA-hexanediol

Table S3. Intracellular dNTP concentrations of *Bordetella* cells (pmol/10^8 cells) as determined by LC-MS/MS

dATP	dGTP	dCTP	TTP	dUTP
21.6 ± 2.4	25.6 ± 1.6	17.7 ± 0.2	18.9 ± 1.4	BLOQ[a]

[a]Below limit of quantification. The limit of dUTP quantification was based on standards to be 0.1 pmol. With an estimate of 4.5 fL per bacterium, a value of 22.5 pmol/10^8 cells is equivalent to 50 µM.

Figure S1

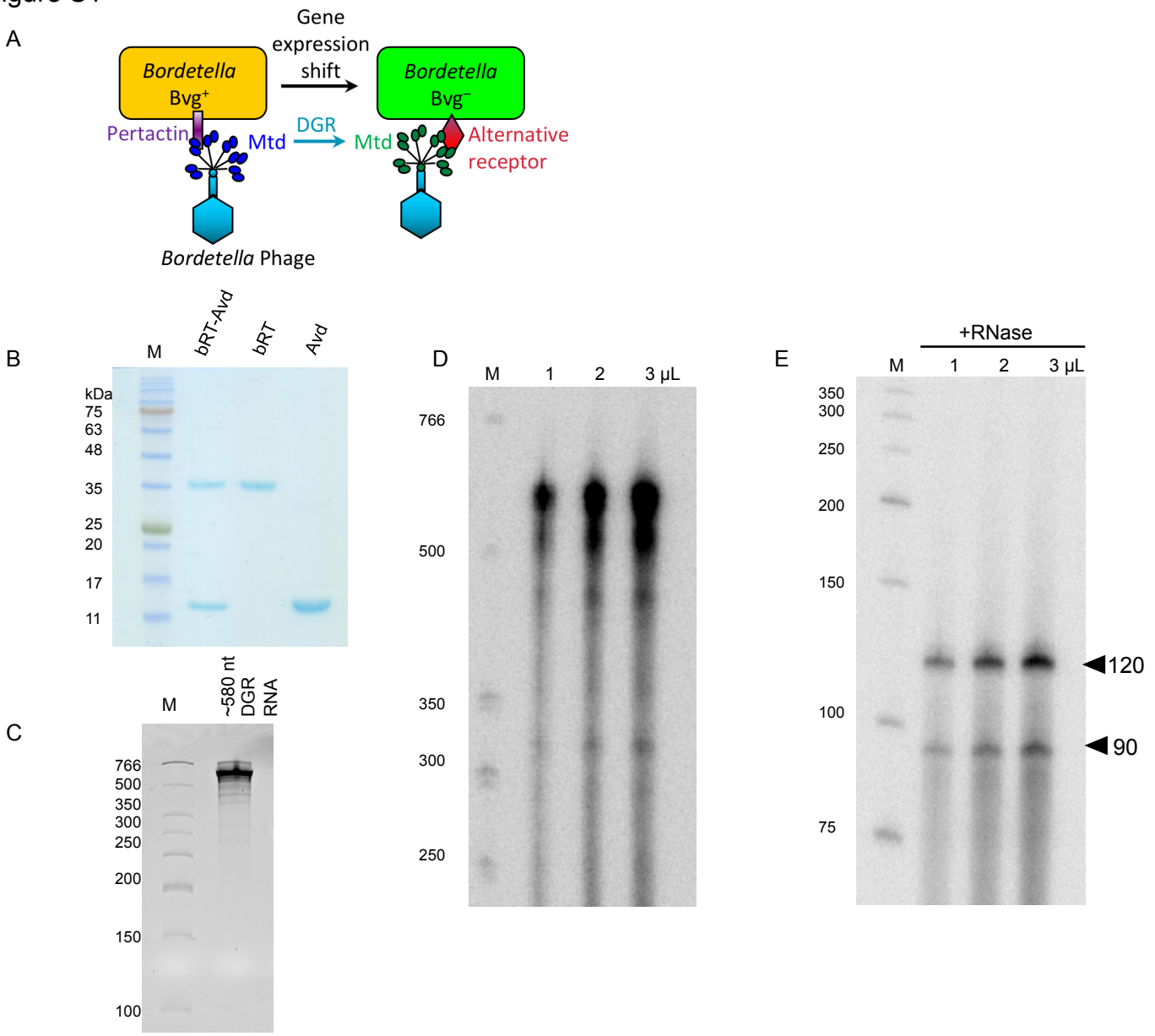

Figure S1. *In vitro* cDNA synthesis.

A. DGR-based variation of Mtd enables *Bordetella* bacteriophage to adapt to changes in surface receptors expressed by its host *Bordetella.*

B. SDS-PAGE of purified bRT-Avd, bRT, and Avd. Lane M corresponds to molecular mass markers.

C. Denaturing polyacrylamide gel (6%) of purified 580 nt DGR RNA. Lane M corresponds to single-stranded DNA molecular mass markers.

D. Increasing quantities of radiolabeled products resulting from the activity of bRT-Avd with the 580 nt DGR RNA as template for 2 h, as in Figure 1C, resolved by 4% denaturing polyacrylamide gel electrophoresis (PAGE).

E. Increasing quantities of radiolabeled products resulting from the activity of bRT-Avd with the 580 nt DGR RNA as template for 2h, following RNase treatment, as in Figure 1C, resolved by 8% denaturing PAGE. Equal quantities were loaded on this gel and the gel in panel S1C. The positions of the 120 and 90 nt cDNAs indicated.

Figure S1 continued

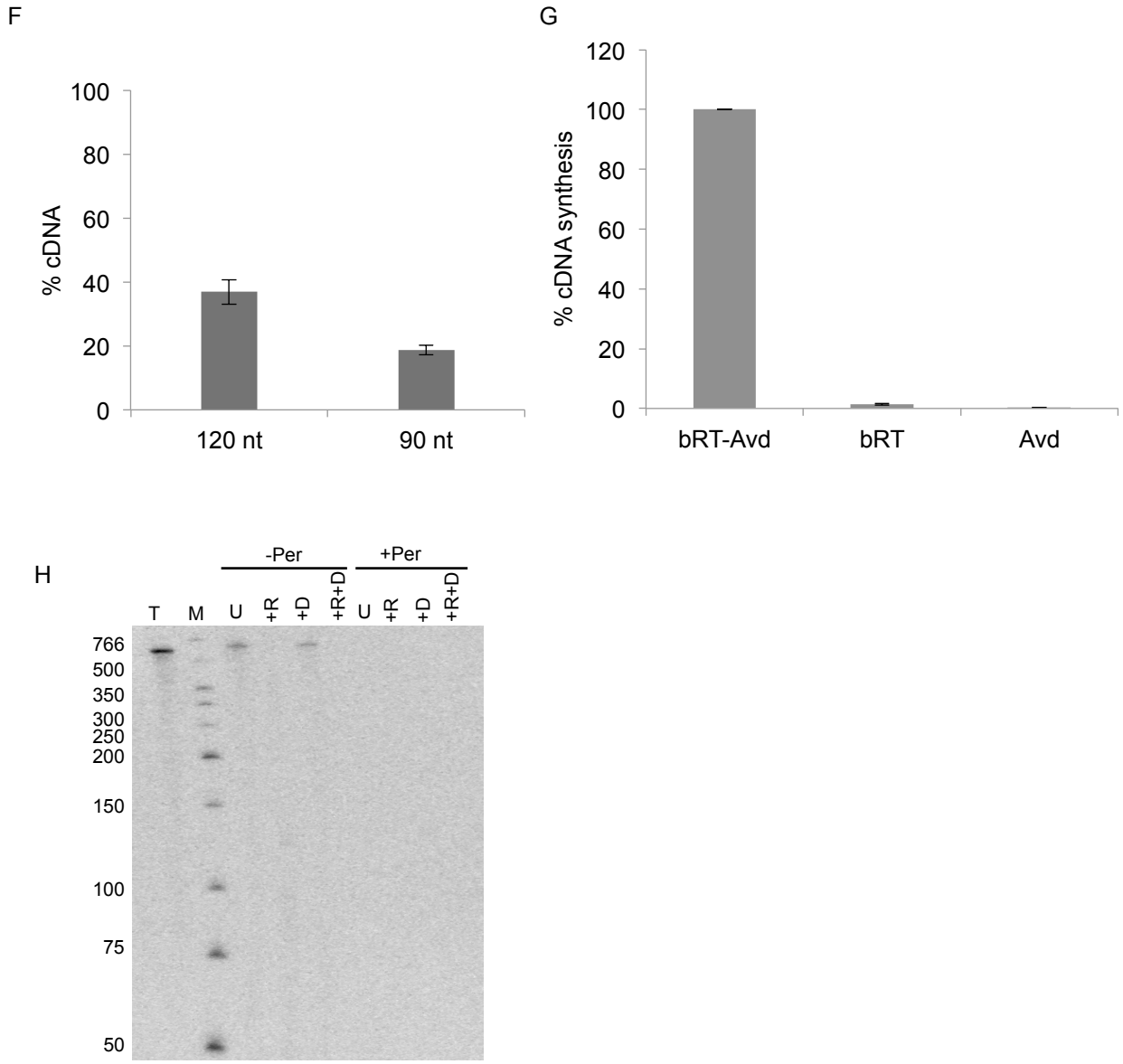

Figure S1 continued. *In vitro* cDNA synthesis.
F. Quantification of radiolabeled 120 and 90 nt bands after 2 h reaction with bRT-Avd and with the 580 nt DGR RNA as template, as a percentage of total radiolabeled products. Means and standard deviations from three independent experiments shown.
G. Quantification cDNA synthesis activity after 2 h reaction with bRT-Avd and with the 580 nt DGR RNA as template (sum of intensity of 120 and 90 nt radiolabeled bands). Values were normalized to that produced by bRT-Avd. Means and standard deviations from three independent experiments shown.
H. Radiolabeled products resulting from bRT activity for 2 h with the 580 nt DGR RNA as template. The 580 nt DGR RNA template was either untreated (-Per) or treated with periodate (+Per) prior to the reverse transcription reaction. Products from the reaction were untreated (U), RNase-treated (+R), DNase-treated (+D), or RNase- and DNase-treated, and resolved by 8% denaturing PAGE.

Figure S2

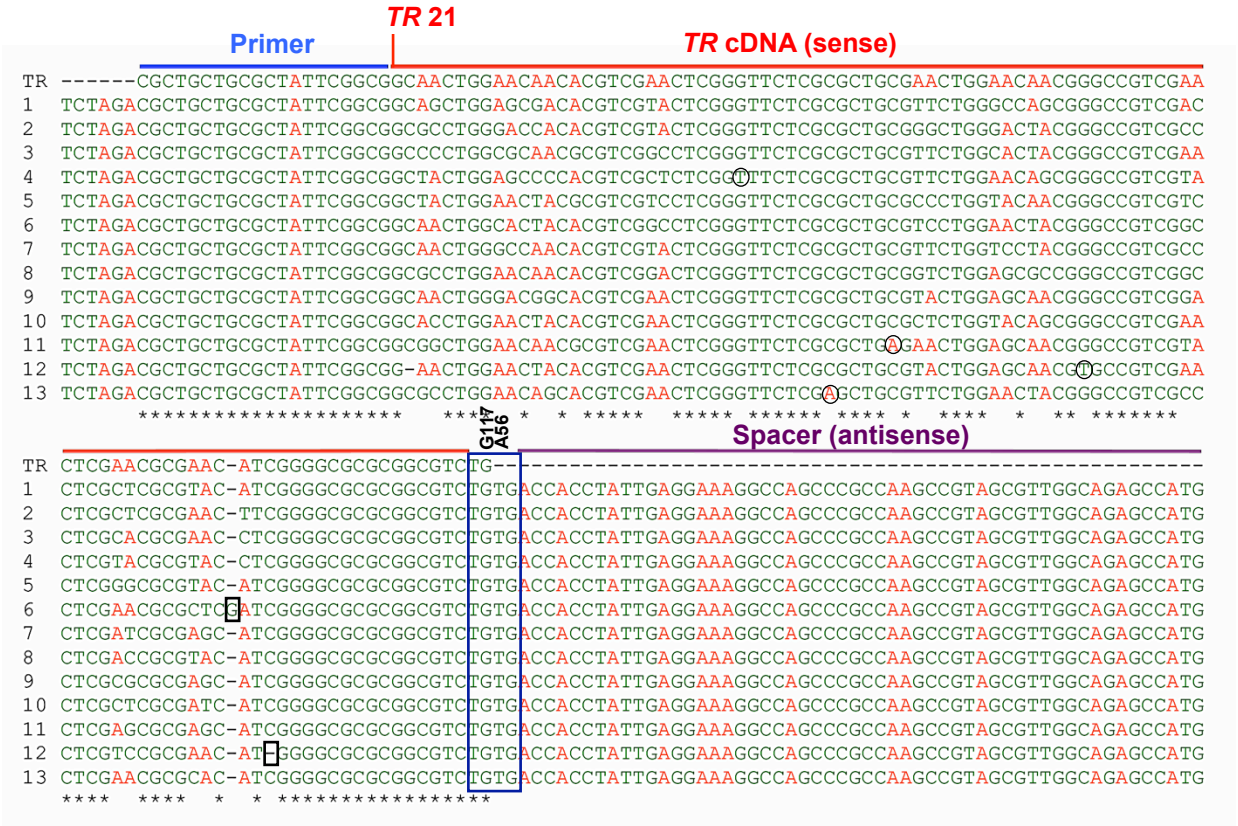

Figure S2. cDNA Sequences.
Sequence of RT-PCR products amplified using primers 1 and 2 (Figure 2A) resulting from bRT-Avd activity with the 580 nt DGR RNA as template. The sequence of the *TR* sense strand was evident up to the boxed region, after which the sequence of the Sp antisense strand was apparent. Bases in the boxed region can correspond to either *TR* or Sp, an ambiguity that is resolved below. Substitutions at bases other than adenine are circled, and single basepair deletions or insertions are in small boxes (0.1%).

Figure S3

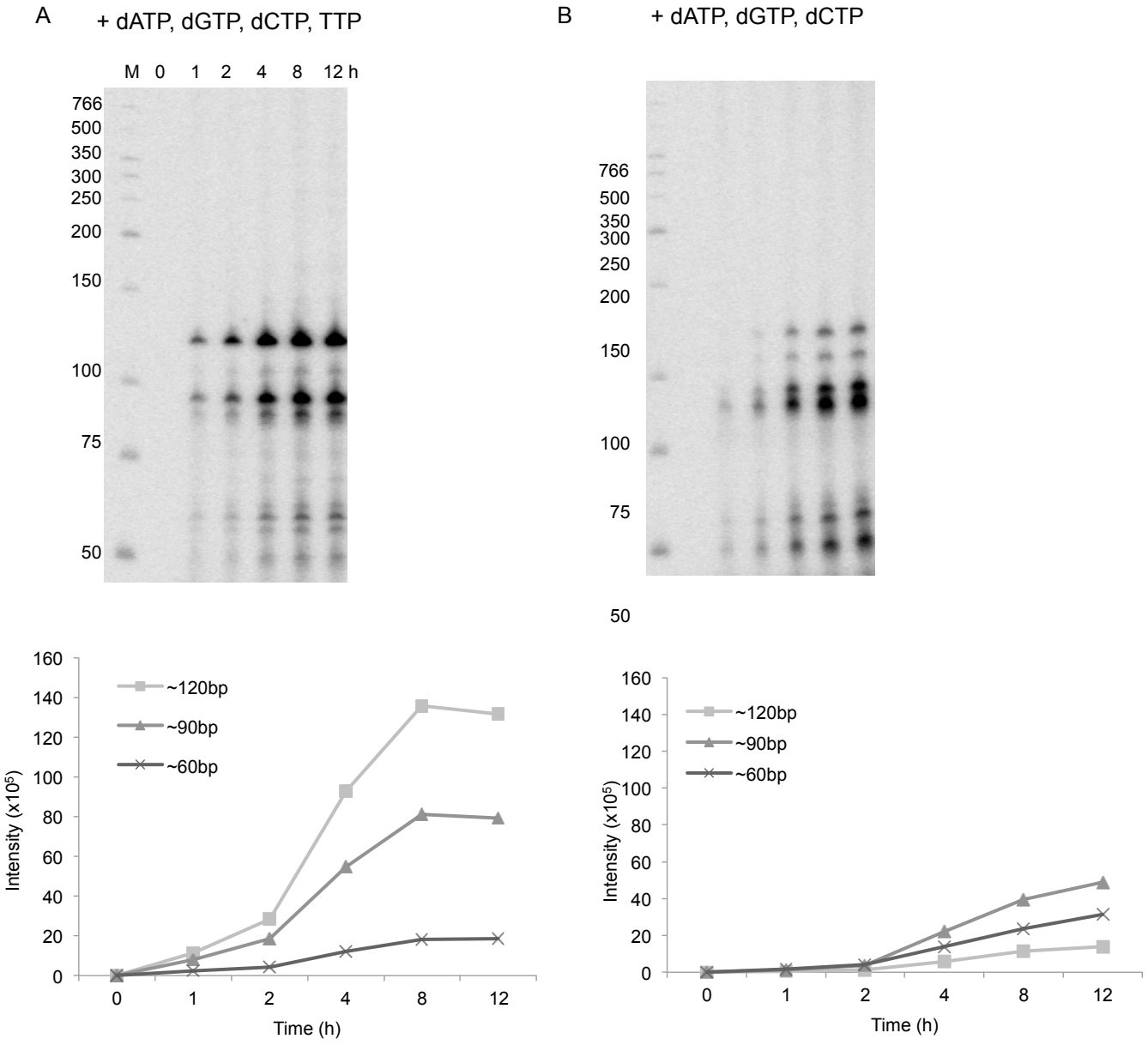

Figure S3. Kinetics of template-primed cDNA synthesis.

A. Top, Radiolabeled cDNA products resulting from bRT-Avd activity for varying times with with the 580 nt DGR RNA as template and in the presence of standard dNTPs. Products were treated with RNase, and resolved by denaturing PAGE. Bottom, Quantification of 60, 90, and 120 nt bands from the gel.

B. Top, Radiolabeled cDNA products resulting from bRT-Avd activity for varying times with the 580 nt DGR as template and in the presence of standard dNTPs but lacking TTP. Products were treated with RNase, and resolved by denaturing PAGE. Bottom, Quantification of 60, 90, and 120 nt bands from the gel.

Figure S4

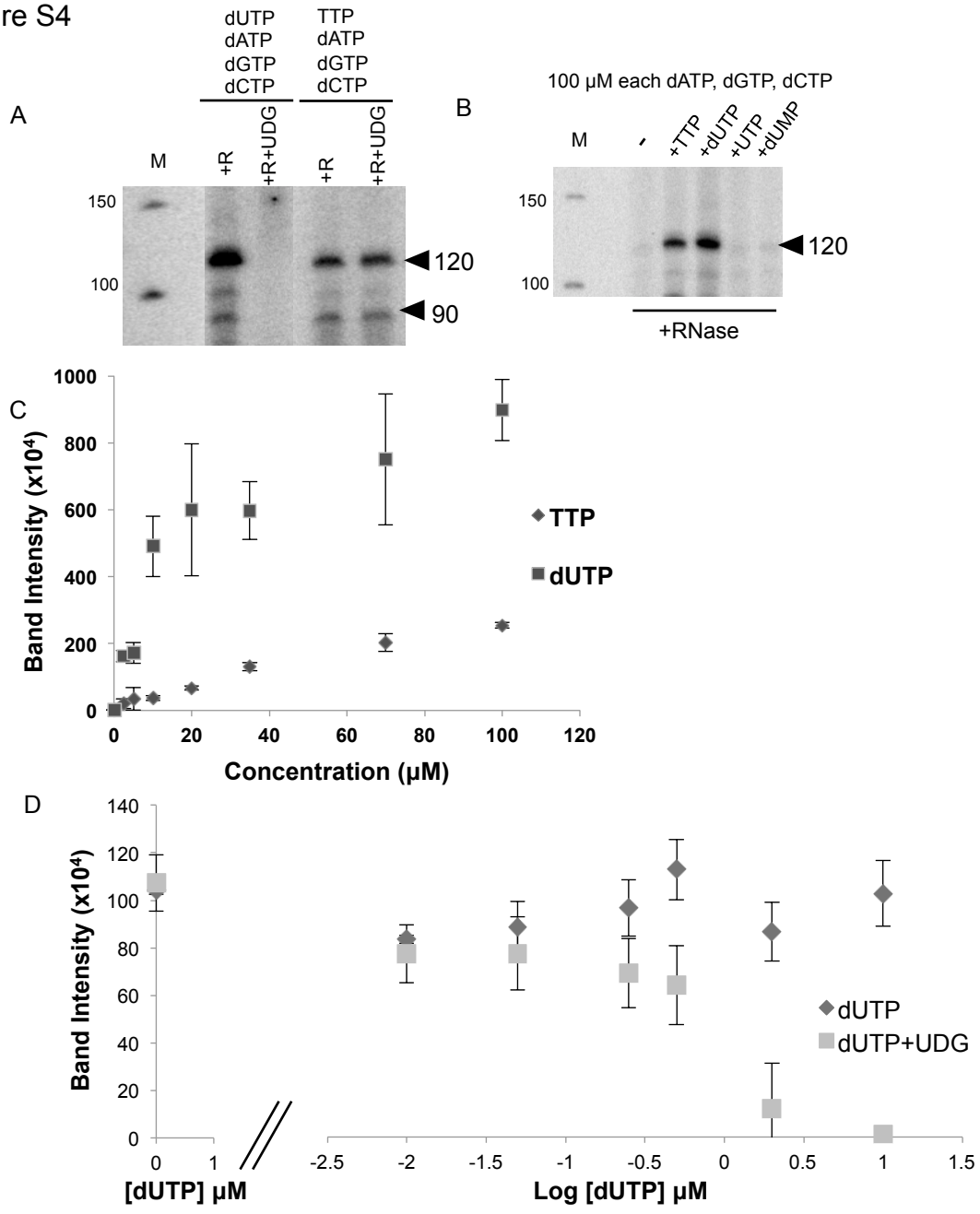

Figure S4. Nucleotide Promiscuity.

A. Radiolabeled cDNA products resulting from bRT-Avd activity for 2 h with the 580 nt DGR RNA as template and in the presence of 100 µM each dATP, dGTP, dCTP, and dUTP (left) or 100 µM each dATP, dGTP, dCTP, and TTP (right). Samples were treated with RNase (R+) or both RNase and UDG (+R+UDG), and resolved by denaturing PAGE.

B. Radiolabeled cDNA products resulting from bRT-Avd activity for 2 h with the 580 nt DGR RNA as template and in the presence of 100 µM each dATP, dGTP, and dCTP, and either no additional component (-), or 100 µM TTP, dUTP, UTP, or dUMP. Samples were treated with RNase, and resolved by denaturing PAGE.

C. Quantification of gel in Figure 2E. Means and standard deviations from three independent experiments are shown.

D. Quantification of gel in panel 2F. Means and standard deviations from three independent experiments are shown.

Figure S4 continued

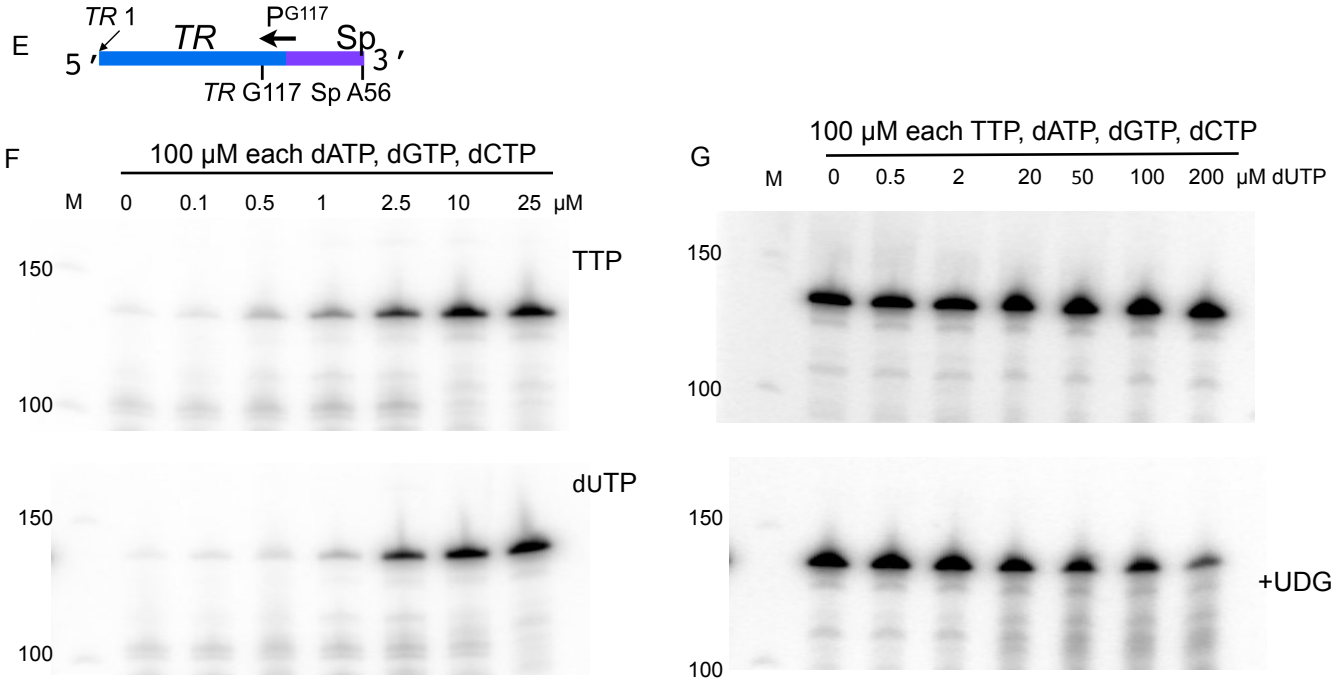

Figure S4 continued. Nucleotide Promiscuity.
E. DGR RNA template used for nucleotide promiscuity experiments with HIV-1 RT, and the oligodeoxynucleotide (ODN) primer P^{G117} that initiates cDNA synthesis with *TR* G117 being the first nucleotide reverse transcribed.
F. Radiolabeled cDNA products resulting from HIV-1 RT activity for 30 min with the DGR RNA template shown in panel S4E and primer P^{G117}, with varying TTP (top) or dUTP (bottom) concentrations. Products were resolved by denaturing PAGE.
G. Radiolabeled cDNA products resulting from HIV-1 RT activity for 30 min with the DGR RNA template shown in panel S4E and primer P^{G117}, with varying dUTP concentrations. Products were untreated (top) or treated with UDG (bottom), and resolved by denaturing PAGE.

Figure S5

A

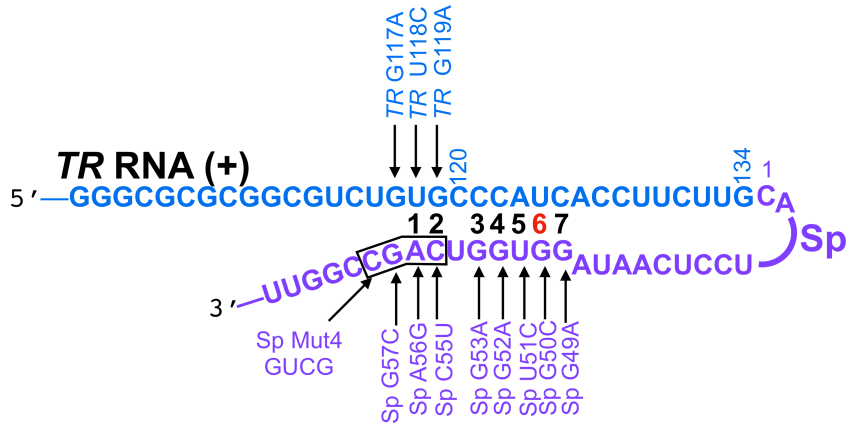

B Sequence observed at *TR*-Sp junction:

GGCGTCTGTGACCACCTATT

Three possibilities for priming and initiation that are consistent with the TGTG (i.e., UGUG in RNA) sequence observed at the *TR*-Sp junction:

1. Priming from Sp A56, with first nucleotide reverse transcribed *TR* G117

```
     TR G117
110 GGCGUCUGUGCCCAUCACCU          Sense TR
          UGACCACCUAUU            Antisense Sp
       56 ACUGGUGGAUAA 45         Sense Sp
          Sp A56
```

2. Priming from Sp C55, with first nucleotide reverse transcribed *TR* U118

```
     TR U118
110 GGCGUCUGUGCCCAUCACCU          Sense TR
          GACCACCUAUU             Antisense Sp
       55 CUGGUGGAUAA 45          Sense Sp
          Sp C55
```

3. Priming from Sp U54, with first nucleotide reverse transcribed *TR* G119

```
     TR G119
110 GGCGUCUGUGCCCAUCACCU          Sense TR
           ACCACCUAUU             Antisense Sp
       54 UGGUGGAUAA 45           Sense Sp
          Sp U54
```

Figure S5. Priming at Sp A56.

A. Substitutions introduced into *TR* and Sp. Potential basepairs numbered (wobble basepair in red).

B. Sequence at the *TR*-Sp junction found from sequencing of RT-PCR amplicons. The pink box denotes the nucleotides that can be assigned to either *TR* or Sp. Following are the three possibilities for priming and initiation sites consistent with the sequencing data.

C

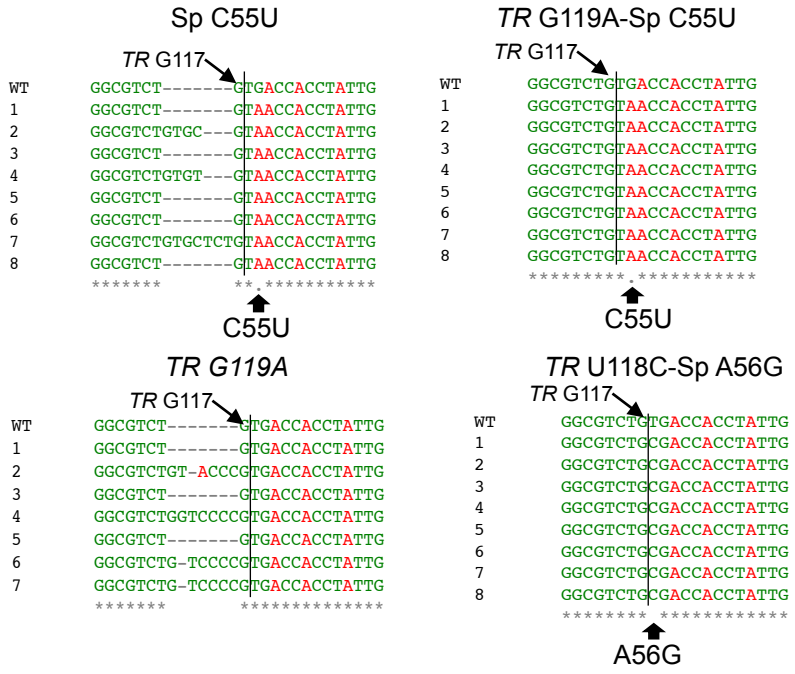

D

Possible Priming Site — Possible Initiation Site	Sp C55U	Sp A56G	*TR* U118C	*TR* G119A
Sp A56 — *TR* G117	+	+	—	—
Sp C55 — *TR* U118	+	—	+	—
Sp U54 — *TR* G119	—	—	+	+

	Sp C55U	Sp A56G	*TR* U118C	*TR* G119A
Observed	+ (Sp C55U, Sp C55U—*TR* G119A)	+ (Sp A56G—*TR* U118C)	— (Sp A56G—*TR* U118C)	— (TR G119A, Sp C55U—*TR* G119A)

Figure S5 continued. Priming at Sp A56.

C. Sequences of RT-PCR products amplified from RNA-cDNA molecules containing substituted templates. Complementary DNA from *TR* T118C could not be amplified and sequenced, likely due to low quantities of cDNA. Substitutions transferred to RT-PCR products are indicated by thick black arrows at the bottom. The vertical line indicates the boundary between TR (left) and Sp (right) deduced from these data.

D. Top, expected pattern of transfer of substitutions to RNA-cDNA molecules for three possibilities of priming and initiation sites shown in panel S5B. "+" indicates transfer of substitution, and "-" lack of transfer. Bottom, the observed pattern of transfer of substitutions indicated that Sp A56 is the priming site and *TR* G117 the first nucleotide reverse transcribed. The substitutions examined to determine the pattern of transfers are indicated in parentheses.

Figure S6

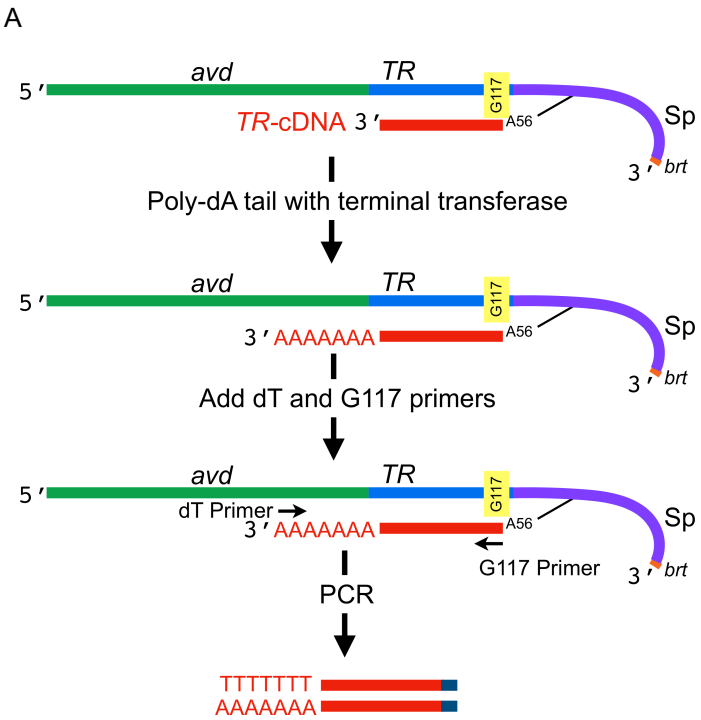

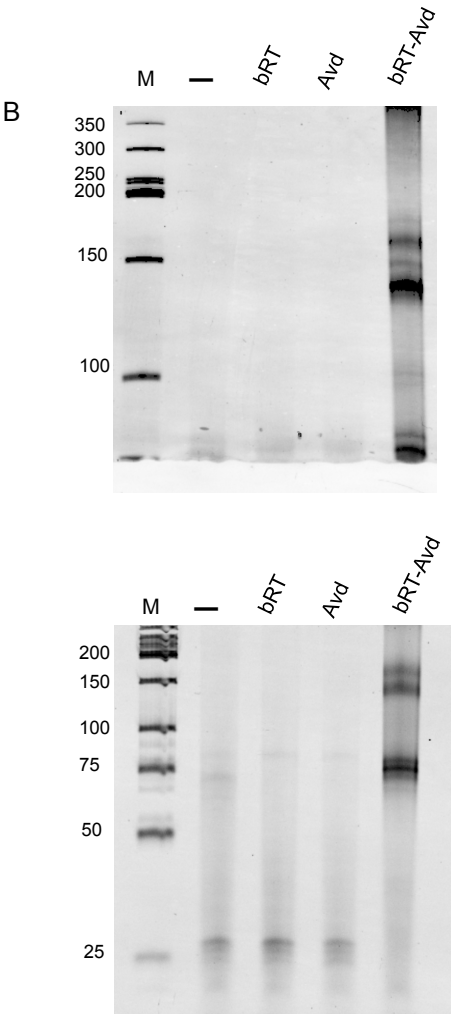

Figure S6. Identification of 3' ends of cDNAs.
A. Schematic for poly-dA tailing and PCR amplification of cDNAs.
B. Products of reverse transcription reactions carried out for 12 h with bRT, Avd, or bRT-Avd were poly-dA tailed and PCR amplified. The products of PCR amplification were resolved and visualized using GreenGlo-stained 10% (top) and 12% (bottom) denaturing PAGE.

Figure S6 continued

C

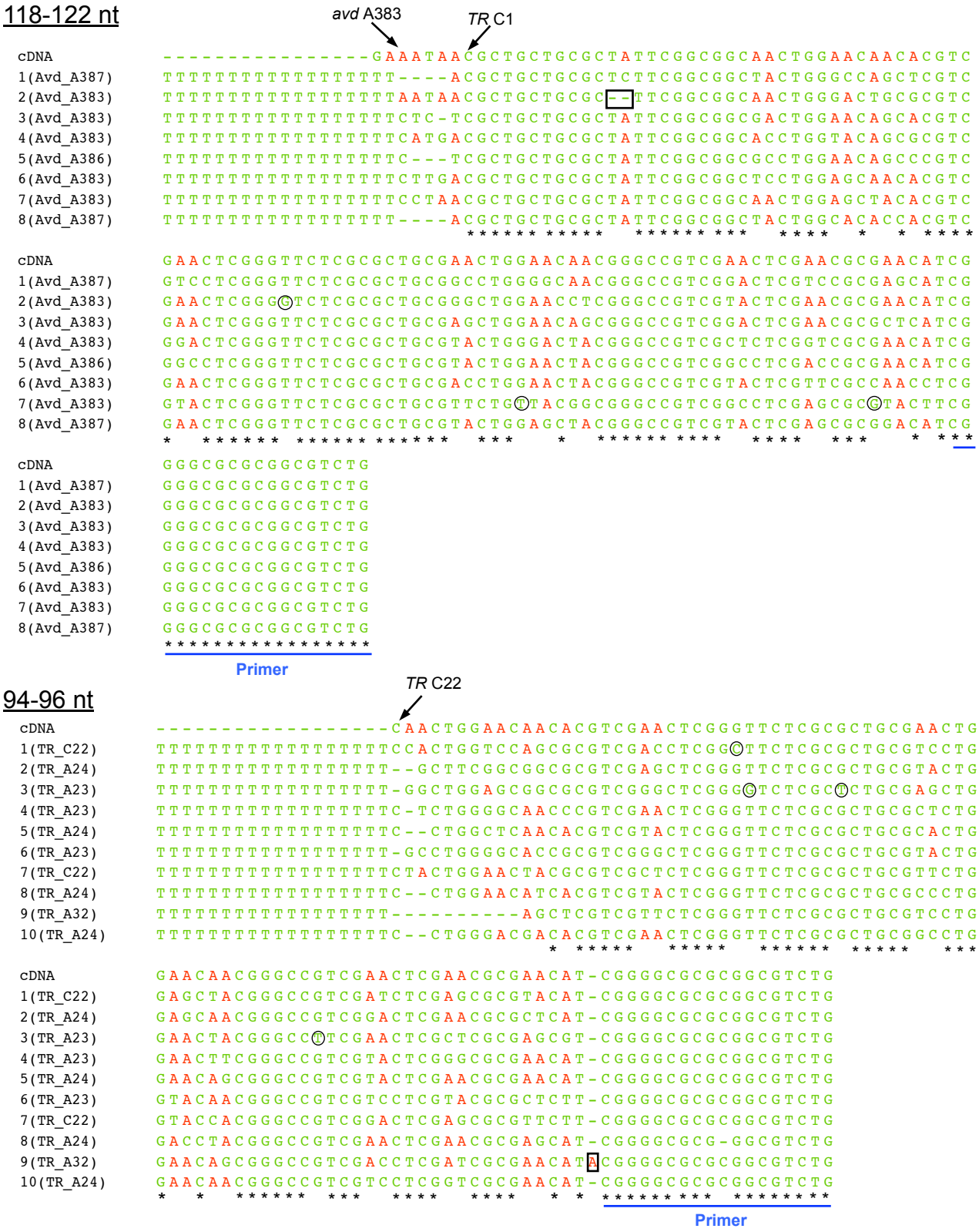

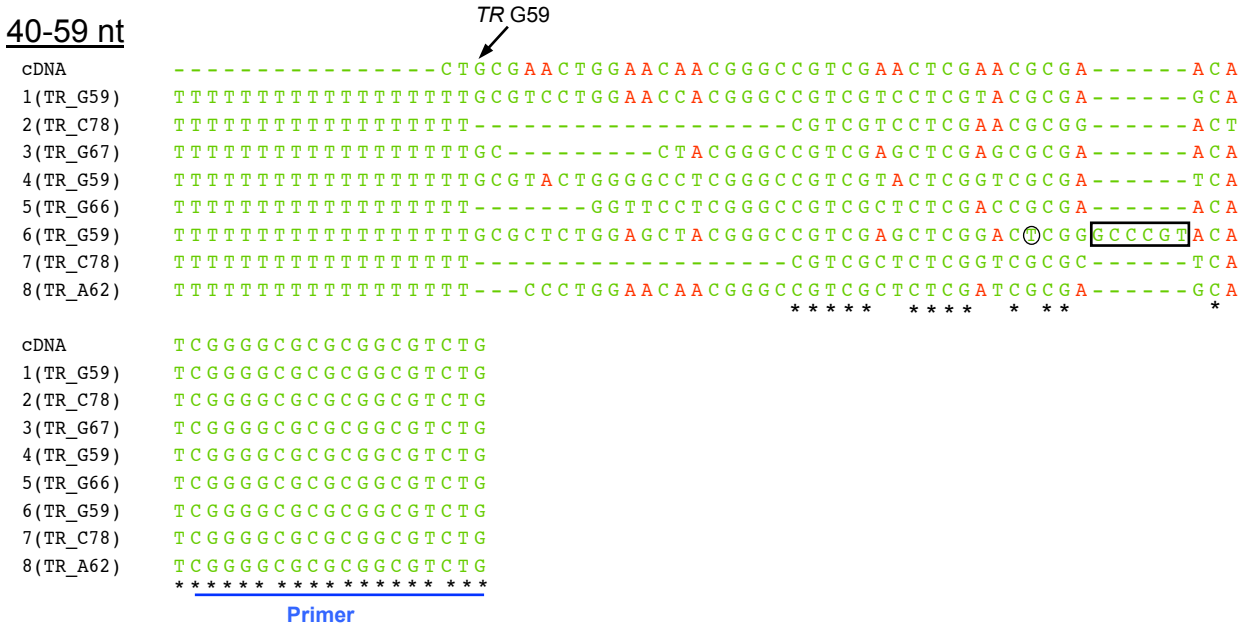

Figure S6 continued. Identification of 3' ends of cDNAs.

C. Sequences of PCR amplicons from panel S6B. Substitutions at bases other than adenine are circled, and deletions or insertions are boxed. Three size classes of cDNAs were identified. Complementary DNAs are denoted by the position in *avd* or *TR* of their 3' base, which immediately follows the sequence of the poly-dT primer. In cases in which an adenine is upstream of the assigned 3' position, it is conceivable that the 3' termination site is one or more nucleotides further upstream of the assigned position, if adenine-mutagenesis had created an A to T substitution at one or more of these upstream adenines. An example is clone 1 (Avd_A387), in which the assigned termination site at 387 could instead be at 386, 385, 384, 383, or 382, depending on whether any of the upstream A's had been mutagenized to T's. The 94-96 nt class includes one cDNA that was even shorter (86 nt). When the content of cytosines is taken into account, the 2:1 ratio between the 120 nt and 90 nt bands, as quantified from the radiolabeled intensity of these bands in Fig. S1D, reflects instead a 1.6:1 ratio between these species.

Figure S7

A

	Basepair	Disrupting Substitution	Complementary Substitution
1.	*TR* U118 – Sp A56	*TR* U118C, Sp A56G, SpMut4	*TR* U118C – Sp A56G
2.	*TR* G119 – Sp C55	*TR* G119A, SpMut4	*TR* G119A – Sp C55U
3.	*TR* C121 – Sp G53	Sp G53A	*TR* C121U – Sp G53A
4.	*TR* C122 – Sp G52	Sp G52A	*TR* C122U – Sp G52A
5.	*TR* A123 – Sp U51	Sp U51C	
6.	*TR* U124 – Sp G50	Sp G50C	
7.	*TR* C125 – Sp G49	Sp G49A	

B

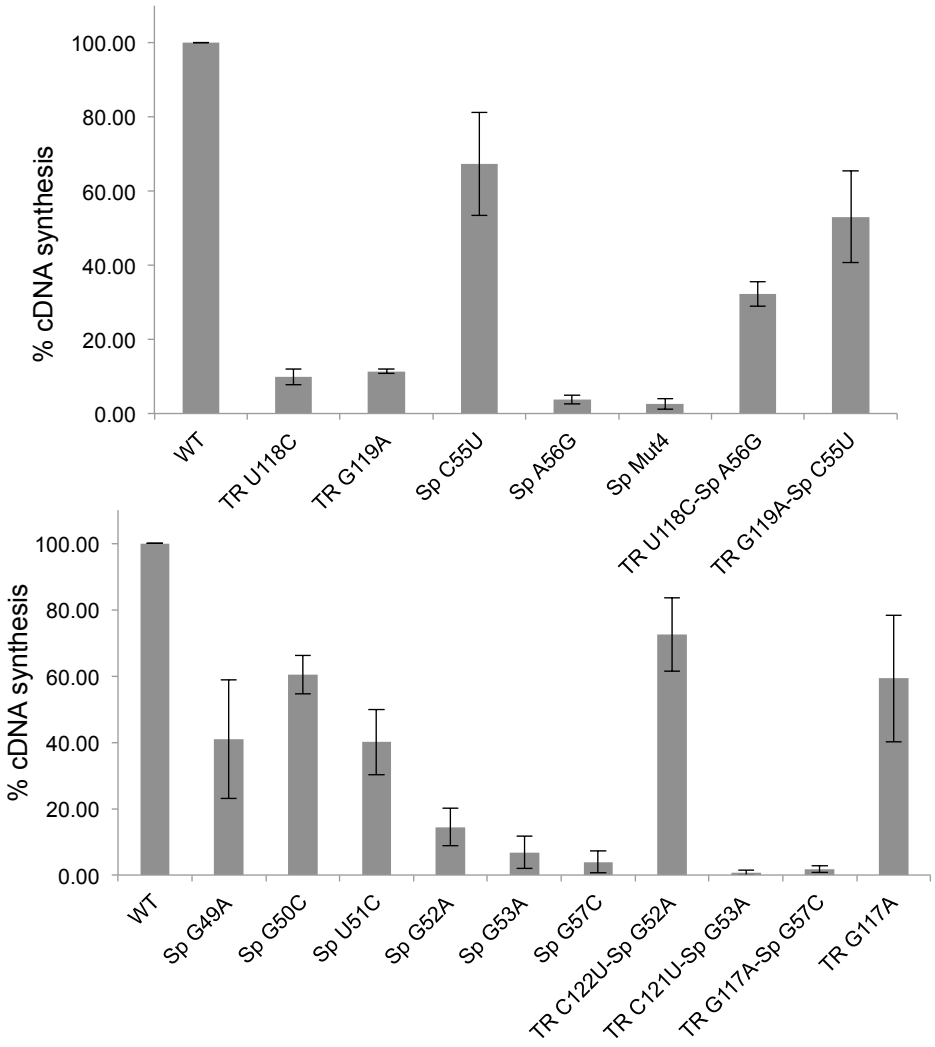

Figure S7. cDNA synthesis from templates substituted in *TR*, Sp, or both.
A. List of possible basepairs between *TR* and Sp, and the disrupting and complementary substitutions introduced into *TR* or Sp.
B. Quantification of radiolabeled cDNA bands (i.e., summed intensities of 90 and 120 nt bands) from the gels in Figure 3B (top and bottom), with values normalized to that produced from the WT DGR template. Means and standard deviations from three independent experiments are shown.

Figure S8

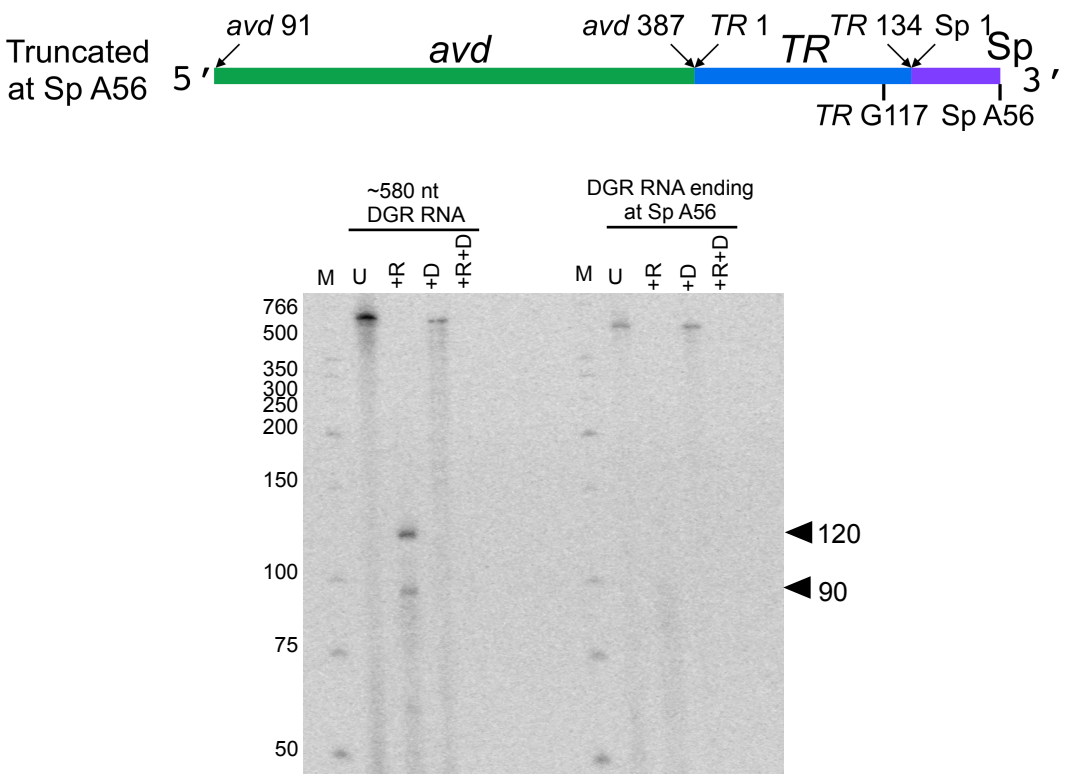

Figure S8. DGR RNA truncated at Sp 56.
Top, schematic of DGR RNA truncated at Sp 56. Bottom, radiolabeled products resulting from bRT-Avd activity with the intact 580 nt DGR RNA or DGR RNA ending at Sp A56 as template. Products were untreated (U), RNase-treated (+R), DNase-treated (+D), or RNase- and DNase-treated (+R+D, and resolved by denaturing PAGE. The positions of the 120 and 90 nt cDNAs are indicated.

Figure S9

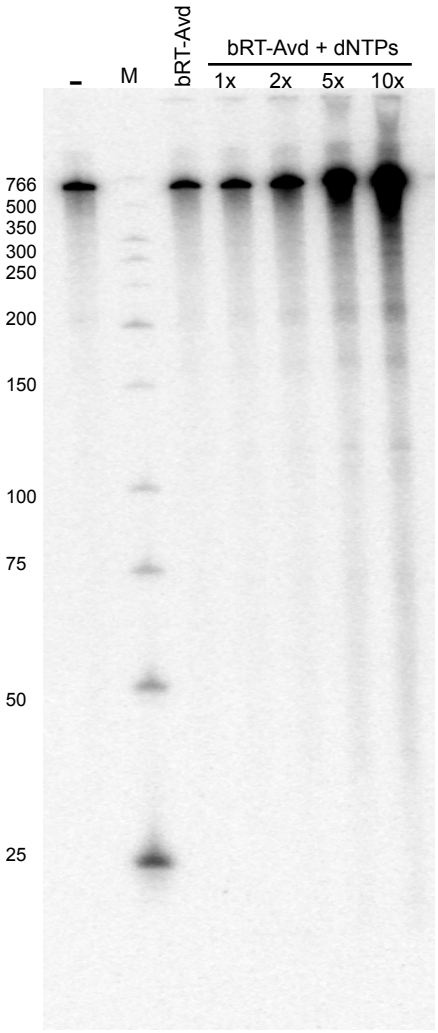

Figure S9. No evidence for cleavage of 580 nt DGR RNA.
Internally-labeled 580 nt DGR RNA was not incubated (–), or incubated with bRT-Avd alone or bRT-Avd with 100 μM standard dNTPs (increasing quantities loaded), and resolved by denaturing PAGE.

Figure S10

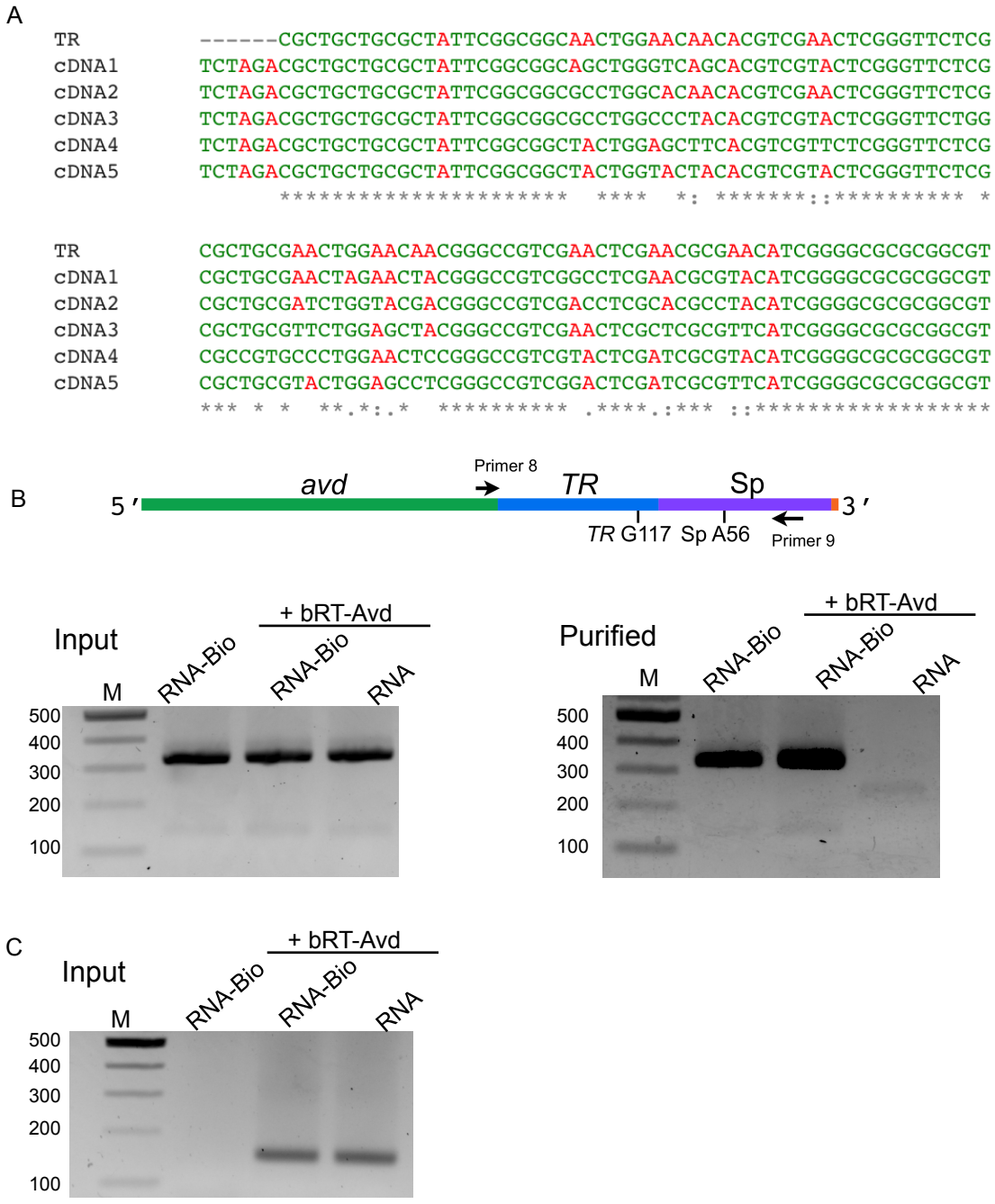

Figure S10. Branched 580 nt RNA-cDNA.

A. Sequences of five PCR products amplified from RNA•biotin-cDNA molecules isolated using streptavidin beads. The reaction was primed with primers 1 and 5 (Table S2), as shown in Figure 4A, and the sequences correspond to *TR*-cDNA.

B. Presence of the 580 nt DGR RNA in samples used in Figure 4B, either before (left, input) or after purification (right) with streptavidin beads, assayed by RT-PCR using primers 8 and 9 (Table S2), as depicted in the schematic above gels.

C. Presence of *TR*-cDNA in samples used in Figure 4B, as detected by PCR using primers shown in Figure 4A, prior to purification using streptavidin beads.

Figure S10 continued

D

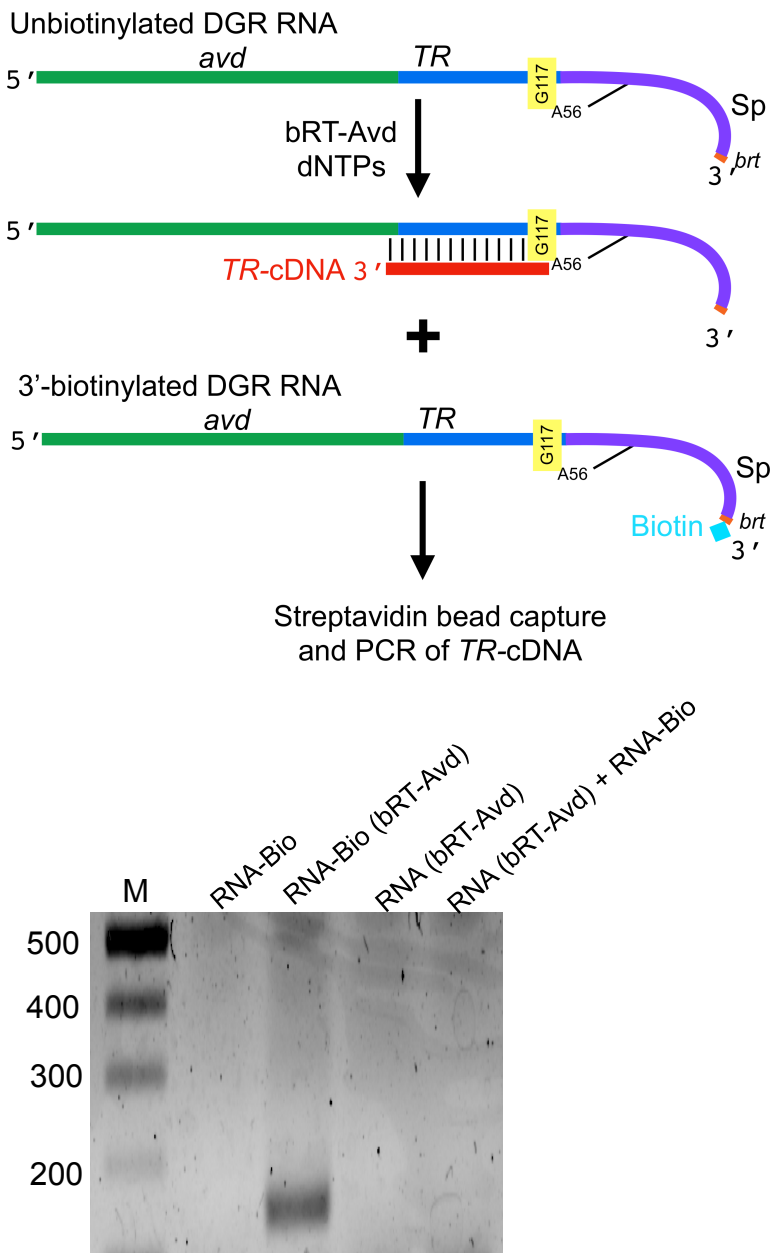

Figure S10 continued. Branched 580 nt RNA-cDNA.
D. Top, schematic of mixing experiment to determine whether RNA-cDNA molecules examined were in *cis*. Bottom, *TR*-cDNA was detected by PCR, as in Figure 4A, for samples isolated with streptavidin beads from 3'-biotinylated 580 nt DGR RNA (RNA-Bio), 3'-biotinylated 580 nt DGR RNA reacted with bRT-Avd (RNA-Bio (bRT-Avd)), unbiotinylated 580 nt DGR RNA reacted with bRT-Avd (RNA (bRT-Avd)), or unbiotinylated 580 nt DGR RNA reacted with bRT-Avd and mixed with biotinylated 580 nt DGR RNA (RNA(bRT-Avd) + RNA-Bio). Products from the PCR reaction were resolved on an agarose gel.

Figure S11

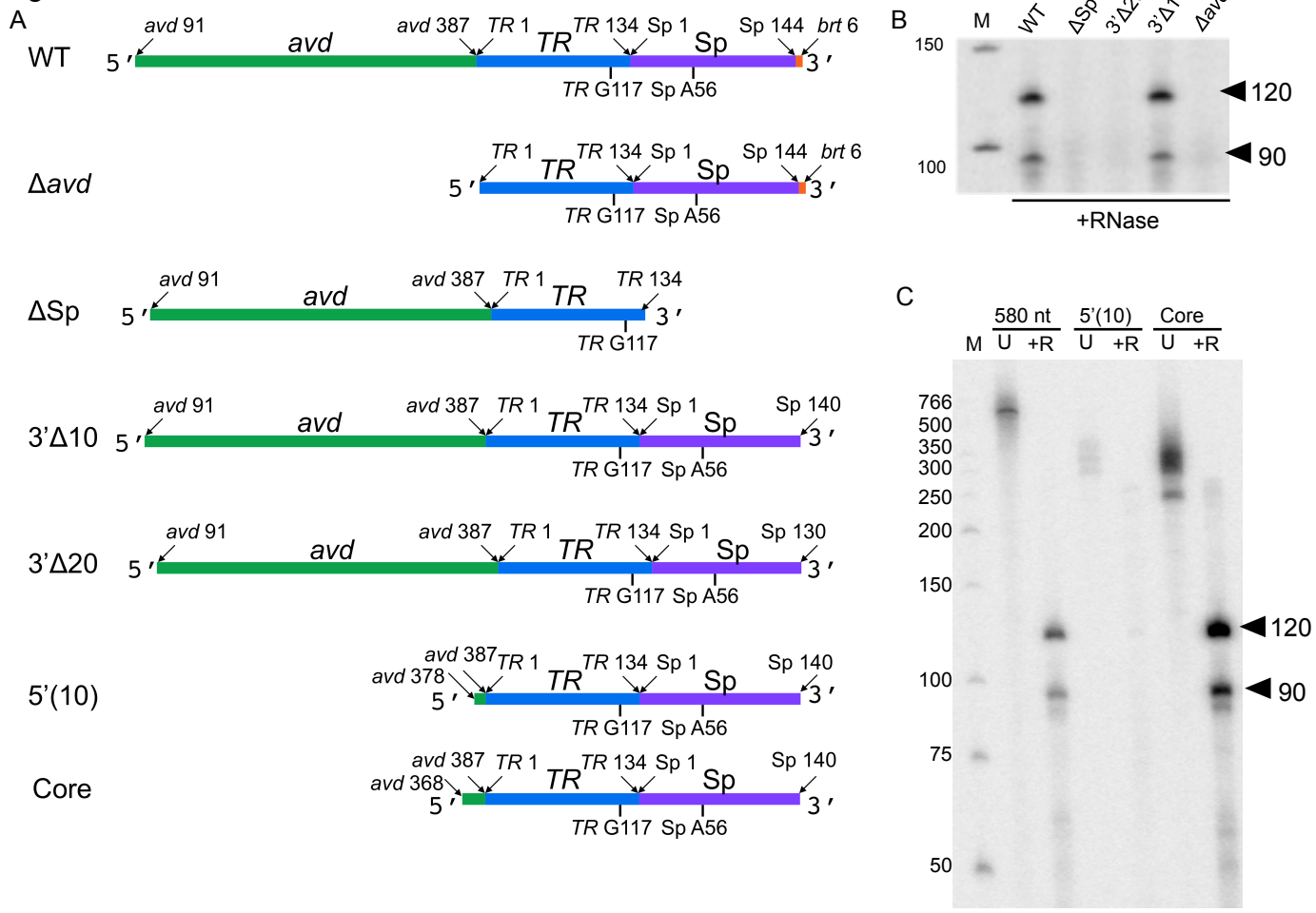

Figure S11. DGR RNA truncations.

A. 5' and 3' truncations of 580 nt DGR RNA.

B. Radiolabeled cDNA products resulting from bRT-Avd activity for 2 h with intact (WT) or truncated DGR RNA as template. Samples were treated with RNase, and resolved by denaturing PAGE. Positions of the 120 and 90 nt cDNAs are indicated.

C. Radiolabeled products resulting from bRT-Avd activity for 2 h with intact 580 nt DGR RNA or truncated DGR RNA as template. Products were untreated (U) or RNase-treated (+R), and [resolved by 8% denaturing PAGE. Positions of the 120 and 90 nt cDNAs are indicated.

Figure S12

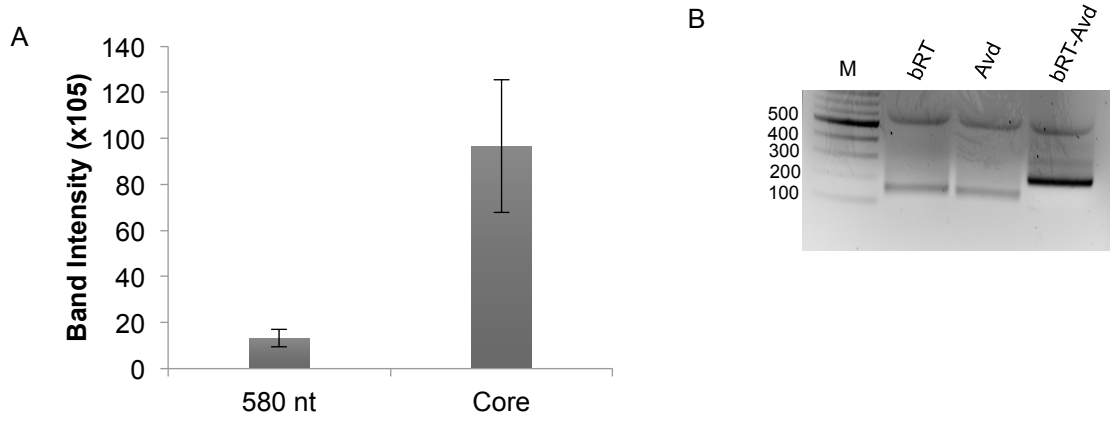

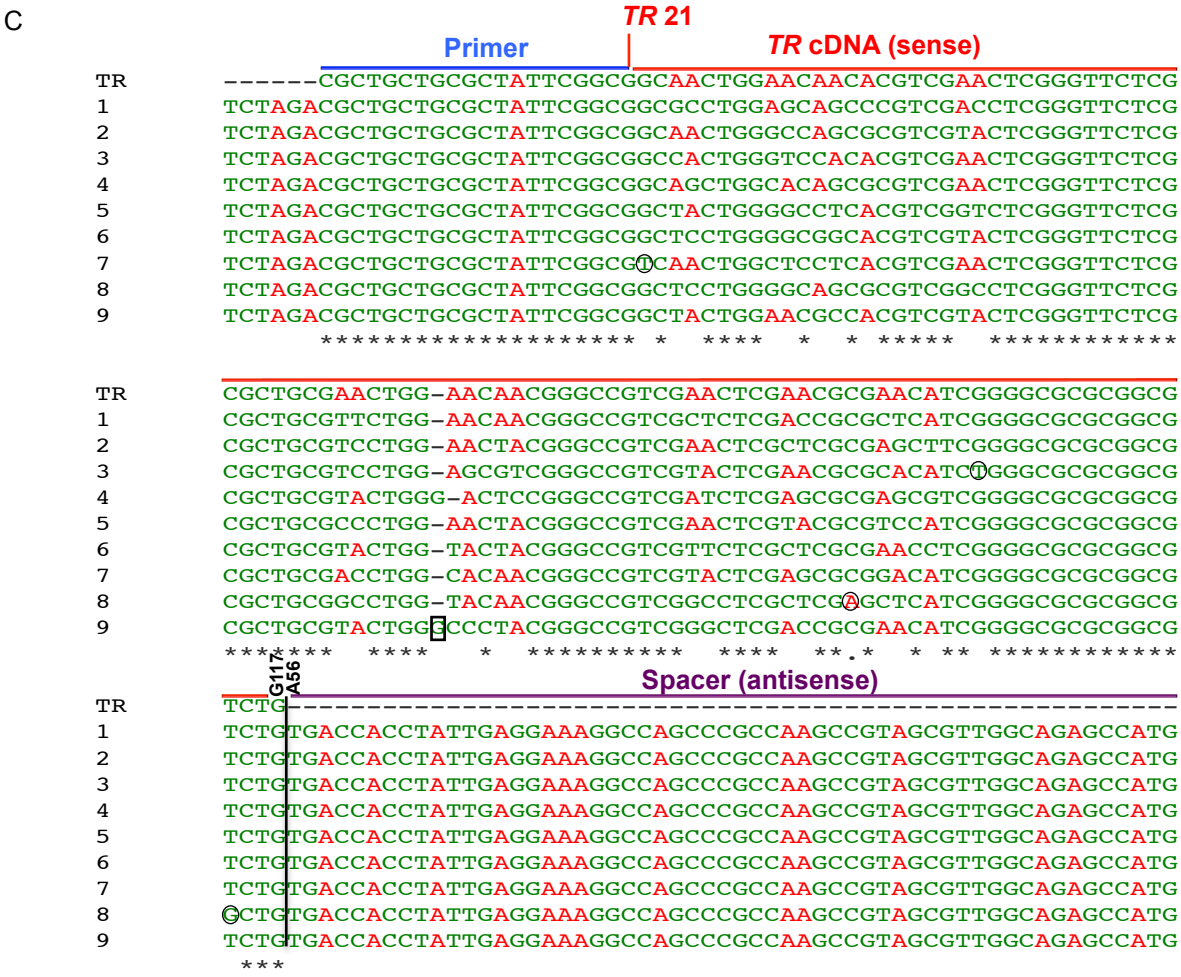

Figure S12. Core DGR RNA.

A. Quantification of cDNA (i.e., summed intensities of 90 and 120 nt bands) produced from 580 nt or core DGR RNA after 2 h of reaction with bRT-Avd. Means and standard deviations from three independent experiments are shown.

B. RT-PCR amplicons from core nt DGR RNA reacted with bRT, Avd, or bRT-Avd, separated on a 2% agarose gel and ethidium bromide-stained.

C. Sequence of RT-PCR products amplified using primers 1 and 2 (Figure 2A) from the core DGR RNA that had been reacted with bRT-Avd and standard dNTPs. Substitutions at bases other than adenine are circled.

Figure S12 continued

D

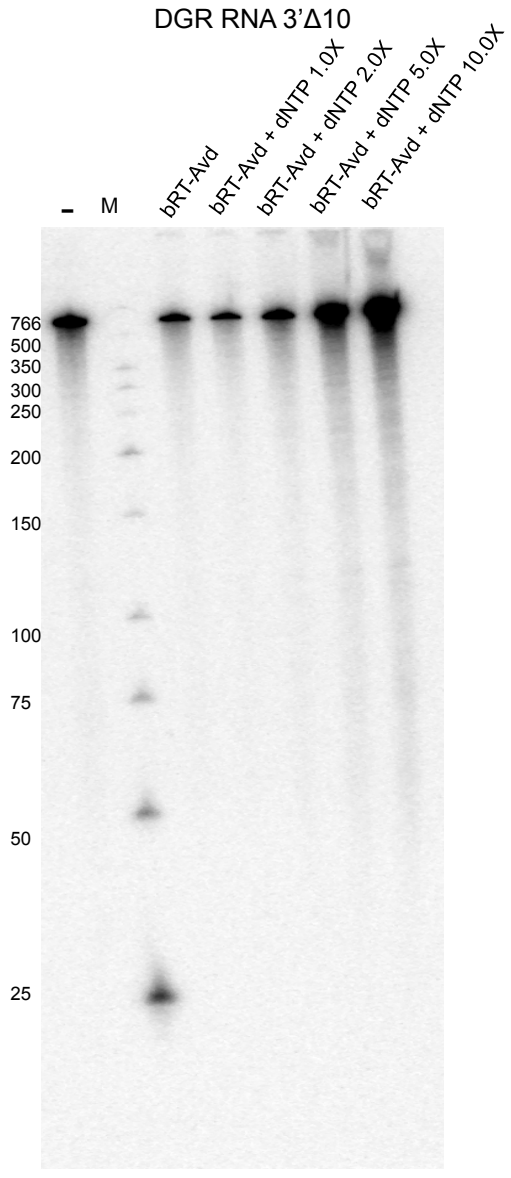

Figure S12 continued. Core DGR RNA.
D. Internally-labeled 3' (Δ10) DGR RNA was not incubated (–), or incubated with bRT-Avd alone or bRT-Avd with 100 μM standard dNTPs (increasing quantities loaded) for 2 h, resolved by denaturing PAGE.

Figure S12 continued

E

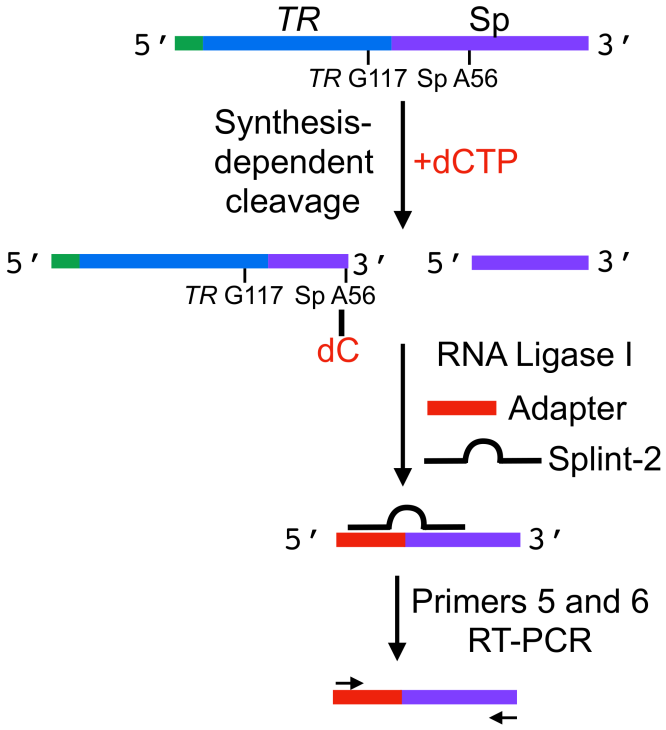

F

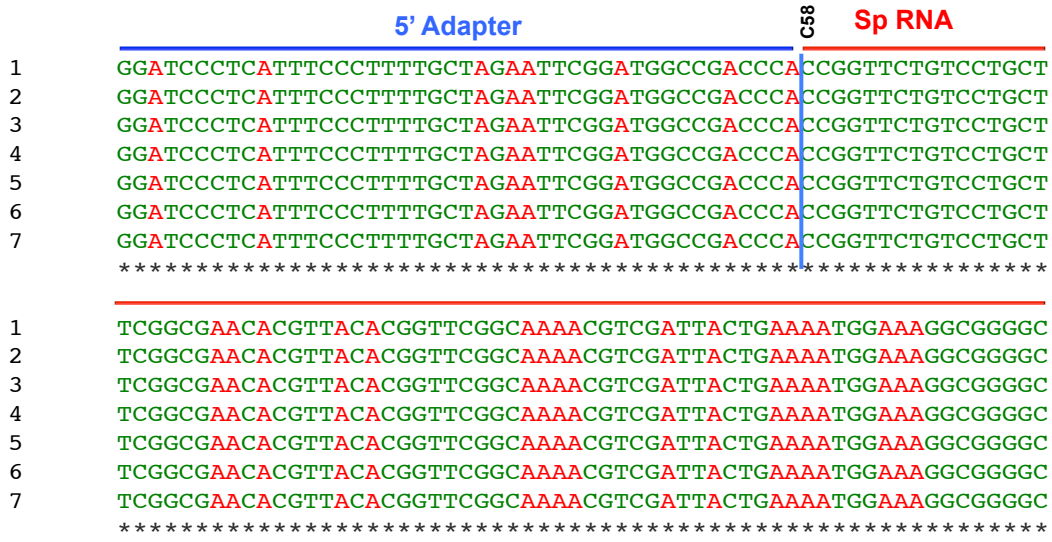

Figure S12 continued. Core DGR RNA.
E. Schematic for RT-PCR of 3' end of cleaved core DGR RNA.
F. Sequence of RT-PCR products amplified from 3' fragment of cleaved core DGR RNA.

G

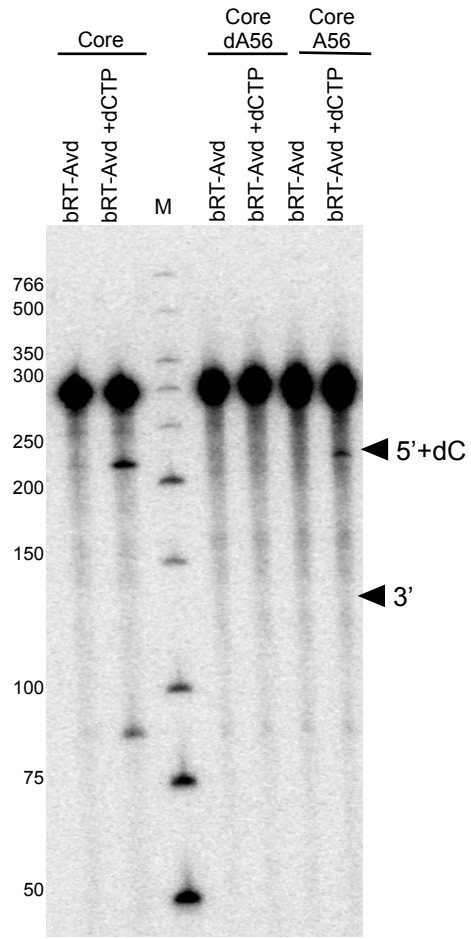

Figure S12 continued. Core DGR RNA.
G. Core, hybrid core dA56, or hybrid core A56 DGR RNA was incubated with bRT-Avd alone or bRT-Avd along with dCTP for 2 h. The core DGR RNA was internally radiolabeled throughout, while only the *in vitro* transcribed portion of hybrid molecules (*avd* 368-Sp 55) were internally radiolabeled. Products from the incubation were resolved by denaturing PAGE. The position of the 5' fragment of cleaved core DGR RNA containing a covalently attached dC is indicated, as is the position of the 3' fragment.

Figure S13

A

```
TR        -------CGCTGCTGCGCTATTCGGCGGCAACTGGAACAACACGTCGAAC-TCGGGTTCTC
cDNA1     TCTAGACGCTGCTGCGCTATTCGGCGGCAACTGGAACAACACGTCGAAC-TCGGGTTCTC
cDNA2     TCTAGACGCTGCTGCGCTATTCGGCGGCTACTGGAACGCCACGTCGGTC-TCGGGTTCTC
cDNA3     TCTAGACGCTGCTGCGCTATTCGGCGGCGCCTGGCTCAACACGTCGCTCGTCGGGTTCTC
cDNA4     TCTAGACGCTGCTGCGCTATTCGGCGGCCCCTGGAGCTTCACGTCGACC-TCGGGTCCTC
cDNA5     TCTAGACGCTGCTGCGCTATTCGGCGGCCACTGGAGCGGCACGTCGAAC-TCGGGTTCTC
                ********************* .****. *  ******* * ****** ***

TR        GCGCTGCGAACTGGAACAACGGGCCGTCGAACTCGAACGCGAACATCGGGGCGCGCGGCG
cDNA1     GCGCTACGTACTGGTCCTACGGGCCGTCGAACTCGTACGCGGGCATCGGGGCGCGCGGCG
cDNA2     GCGCTGCGGCCTGGTACGCCGGGCCGTCGAACTCGAACGCGAACATCGGGGCGCGCGGCG
cDNA3     GCGCTGCGCTCTGGTACTACGGGCCGTCGATCTCGATCGCGTACATCGGGGCGCGCGGCG
cDNA4     GCGCTGCGTCCTGGAACTACGGGCCGTCGGACTCGTACGCGAACATCGGGGCGCGCGGCG
cDNA5     GCGCTGCGTACTGGGGCCTCGGGCCGTCGGCCTCGCTCGCGAACATCGGGGCGCGCGGCG
          *****.**  ****  *  **********. **** :**** .*****************
```

B

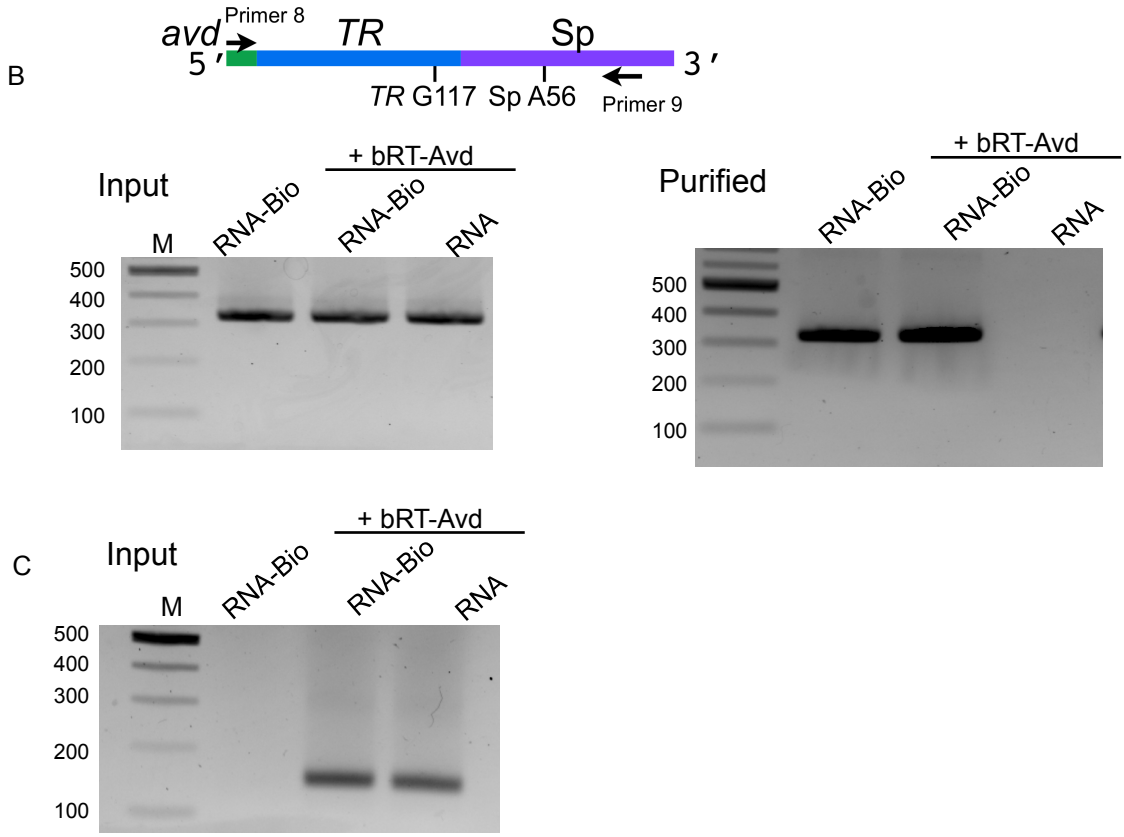

C

Figure S13. Branched core RNA-cDNA.

A. Sequences of five PCR products amplified from RNA•biotin-cDNA molecules isolated using streptavidin beads. The reaction was primed with primers 1 and 5 (Table S2), as shown in Figure 4A, and the sequences correspond to *TR*-cDNA.

B. Presence of the core DGR RNA in samples used in Figure 5D, either before (left, input) or after purification (right) with streptavidin beads, assayed by RT-PCR using primers 8 and 9 (Table S2), as depicted in the schematic above gels.

C. Presence of *TR*-cDNA in samples used in Figure 5D, as detected by PCR using primers shown in Figure 4A, prior to purification using streptavidin beads.

D

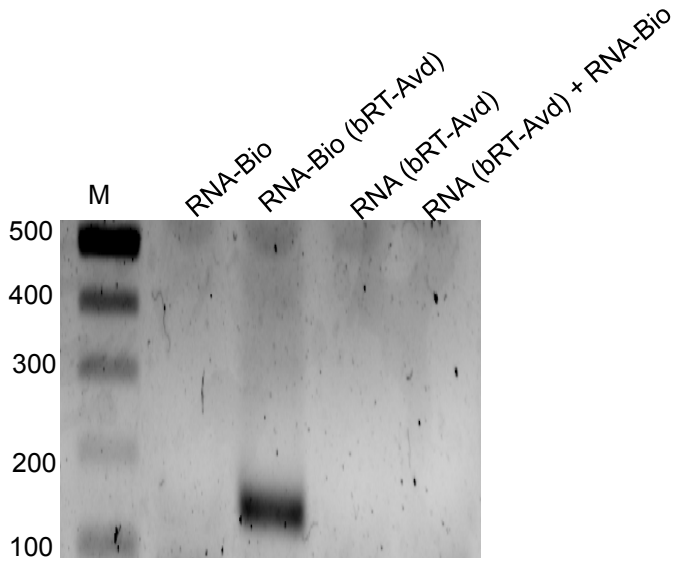

Figure S13 continued. Branched core RNA-cDNA.
D. *TR*-cDNA was detected by PCR, as in Figure 4A, for samples isolated with streptavidin beads from 3'-biotinylated core DGR RNA (RNA-Bio), 3'-biotinylated core DGR RNA reacted with bRT-Avd (RNA-Bio (bRT-Avd)), unbiotinylated core DGR RNA reacted with bRT-Avd (RNA (bRT-Avd)), or unbiotinylated core DGR RNA reacted with bRT-Avd and mixed with biotinylated core DGR RNA (RNA(bRT-Avd) + RNA-Bio). Products from the PCR reaction were resolved on an agarose gel.

Figure S14

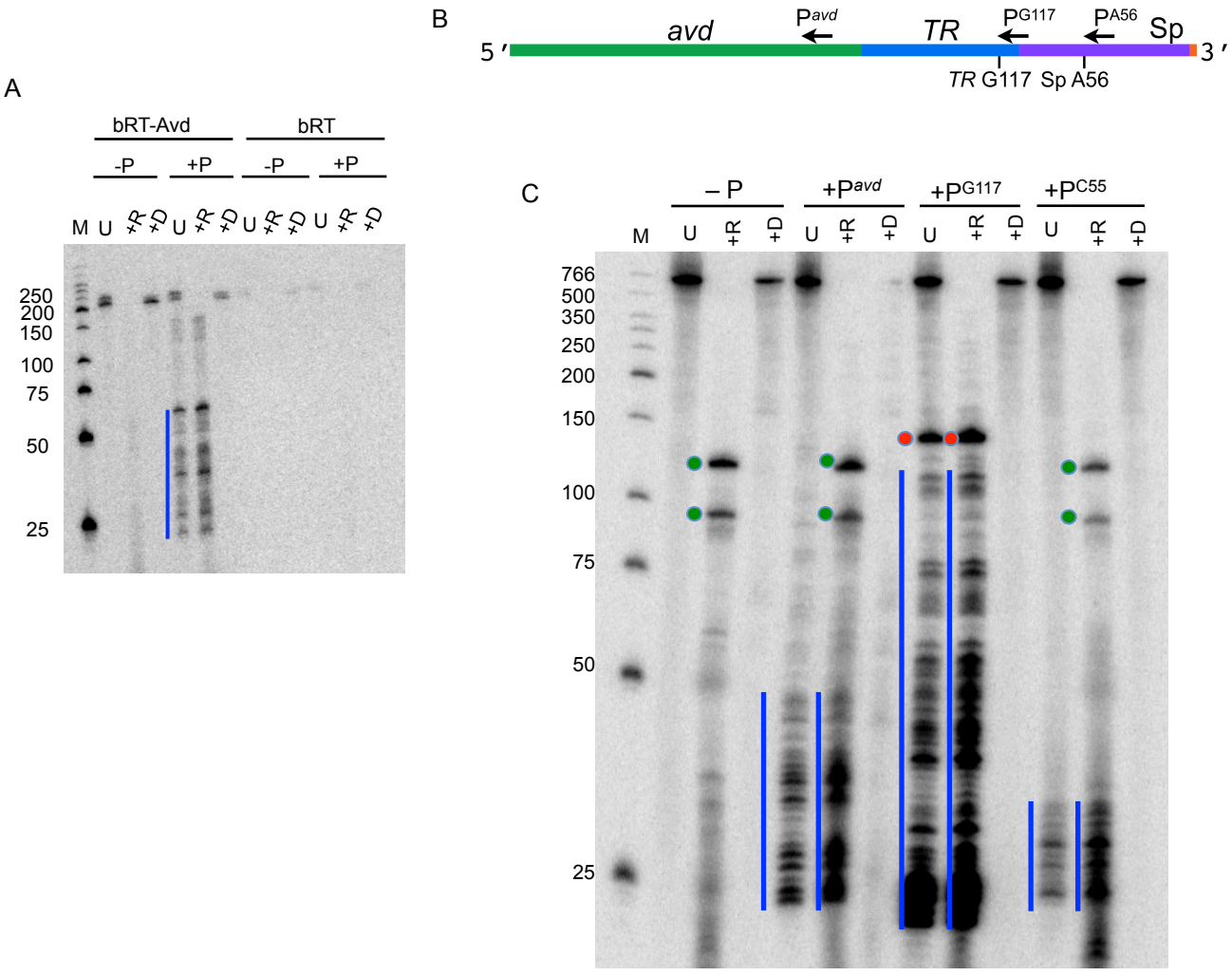

Figure S14. Specificity to DGR RNA.
A. Radiolabeled products resulting from the activity of bRT-Avd or bRT with a non-DGR RNA as template. Either no primer (-P) or an ODN primer (+P) was included. Products were untreated (U), RNase-treated (+R), or DNase-treated (+D), and resolved by 12% denaturing PAGE. The blue lines indicate ODN-primed cDNA products. The cDNAs are 5-35 nt (cDNA + 20 nt primer for 25-55 nt bands).
B. DGR RNA and primers used for reverse transcription reactions (P^{avd}, P^{G117}, and P^{A56}).
C. Radiolabeled products resulting from bRT-Avd activity with the 580 nt DGR RNA as template. Either no primer (-P), or primers P^{avd}, P^{G117}, or P^{A56} were included. Products were untreated (U), RNase-treated (+R), or DNase-treated (+D), and resolved by denaturing PAGE. The blue lines indicate ODN-primed cDNA products. The red dots indicates ODN-primed cDNAs (present in both U and +R lanes) that are ~120 nt in length (cDNA + 20 nt primer for a ~140 nt band), and the green dots are the template-primed cDNAs of 90 and 120 nt (present only in +R lanes).

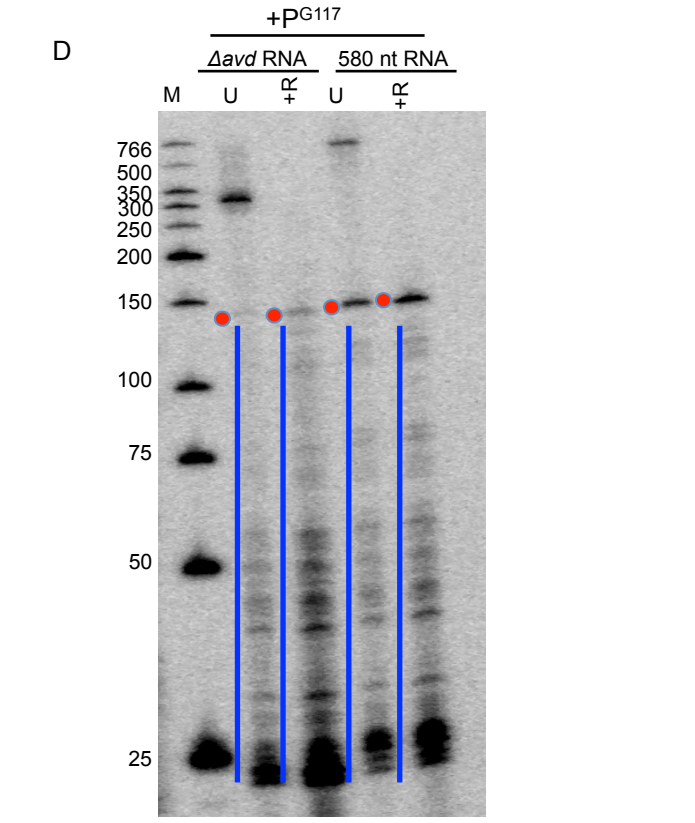

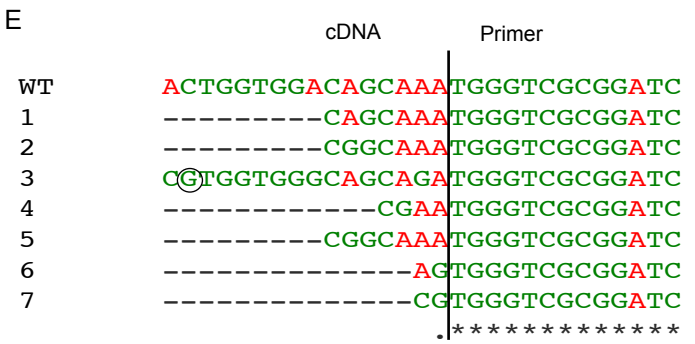

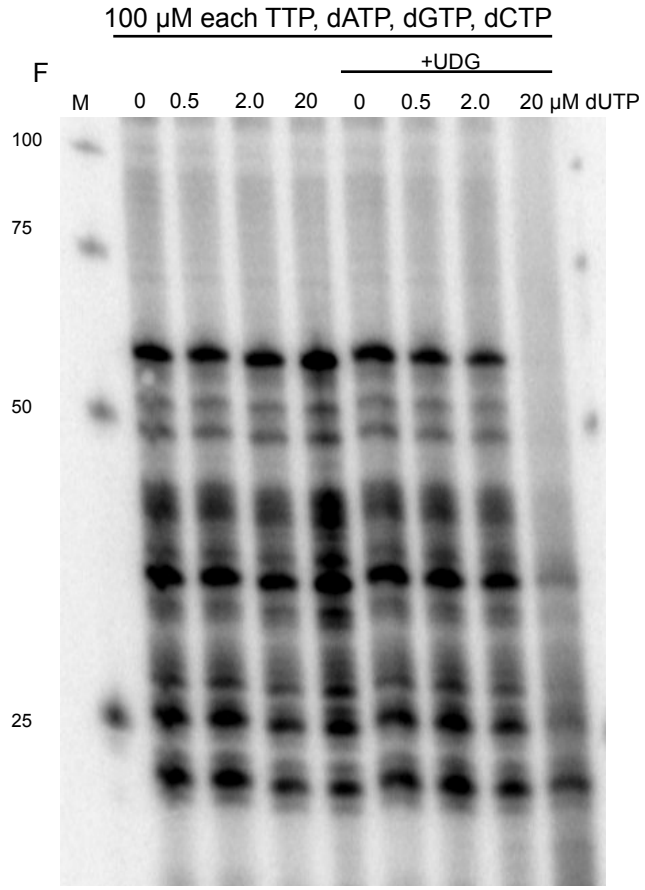

Figure S14 continued. Specificity to DGR RNA.

D. Radiolabeled products resulting from bRT-Avd activity with *Δavd* or 580 nt DGR RNA as template and primer P^{G117}. Products were untreated (U) or treated with RNase (+R)m and resolved by denaturing PAGE. The blue lines indicate ODN-primed cDNA products. The red dots indicates ODN-primed cDNAs that are ~120 nt in length (cDNA + 20 nt primer for a ~140 nt band).

E. Sequence of RT-PCR products generated from the action of bRT-Avd with a non-DGR RNA template, as primed by an ODN (indicated by 'Primer'). The dashes correspond to T's, which were due to poly-dA tailing of the cDNAs prior to amplification. The circle indicates mutagenesis at bases other than adenine.

F. Radiolabeled products resulting from ODN-primed bRT-Avd activity with a non-DGR RNA template, with varying dUTP concentrations. Products were untreated or UDG-treated (+UDG), and resolved by denaturing PAGE.

Figure S15

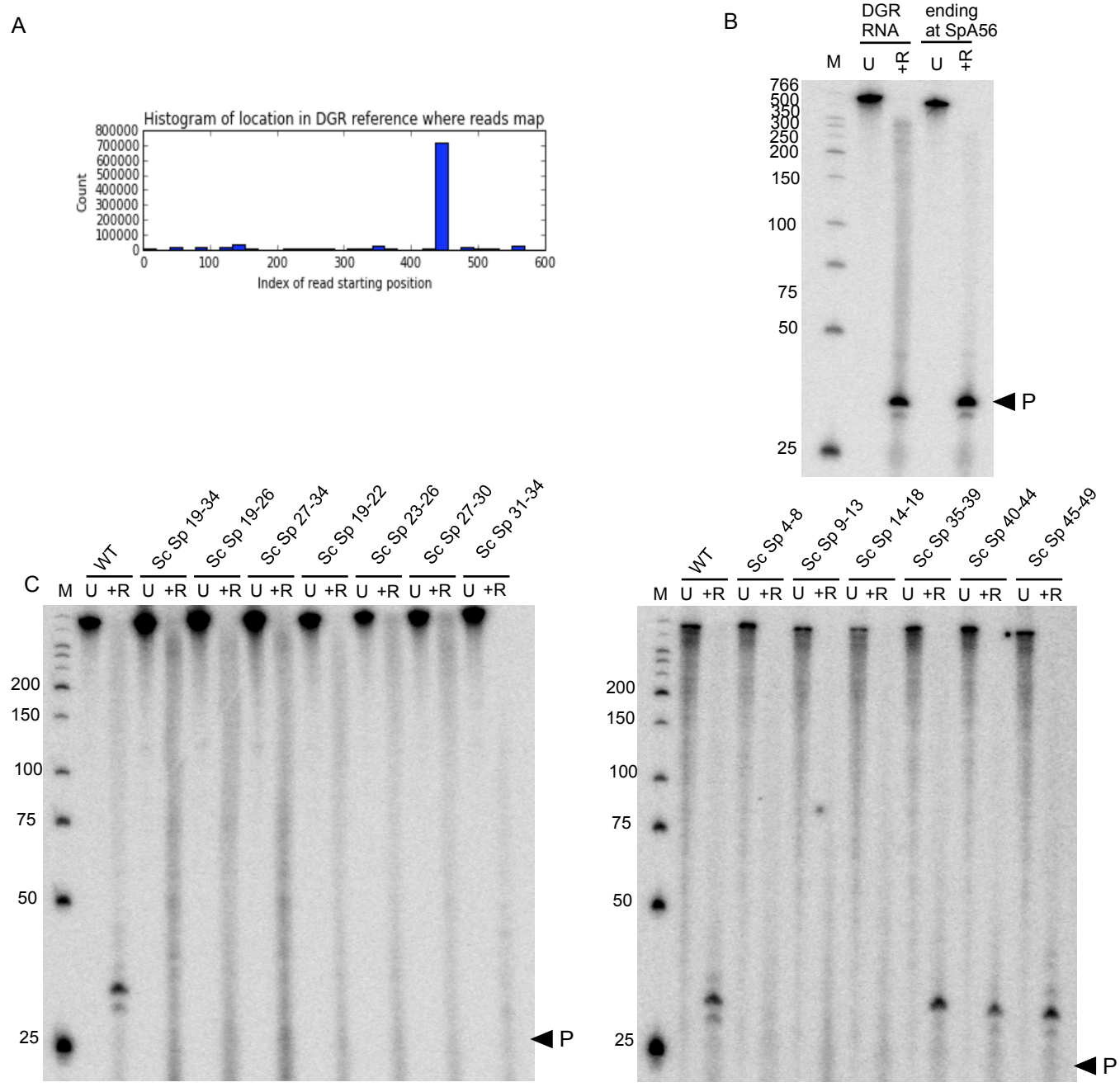

Figure S15. RNase protection.

A. Illumina small RNA sequencing results of RNA fragmented protected from RNase digestion by Avd. Count of the sequencing result was plotted with respect to the DGR RNA sequence.

B. RNase protection by Avd carried out on internally-labeled 580 nt DGR RNA, wild-type or truncated at Sp 56. Samples were either untreated (U) or RNase-treated (+R), and resolved by denaturing PAGE. The position of the protected (P) band is indicated.

C. RNase protection by bRT-Avd carried out on internally-labeled 580 nt DGR RNA, wild-type or with scrambled (Sc) Sp sequences. The first lane in each pair was untreated (U) and the second RNase-treated (+R), and resolved by denaturing PAGE. The position of the protected (P) band is indicated.

Figure S15 continued

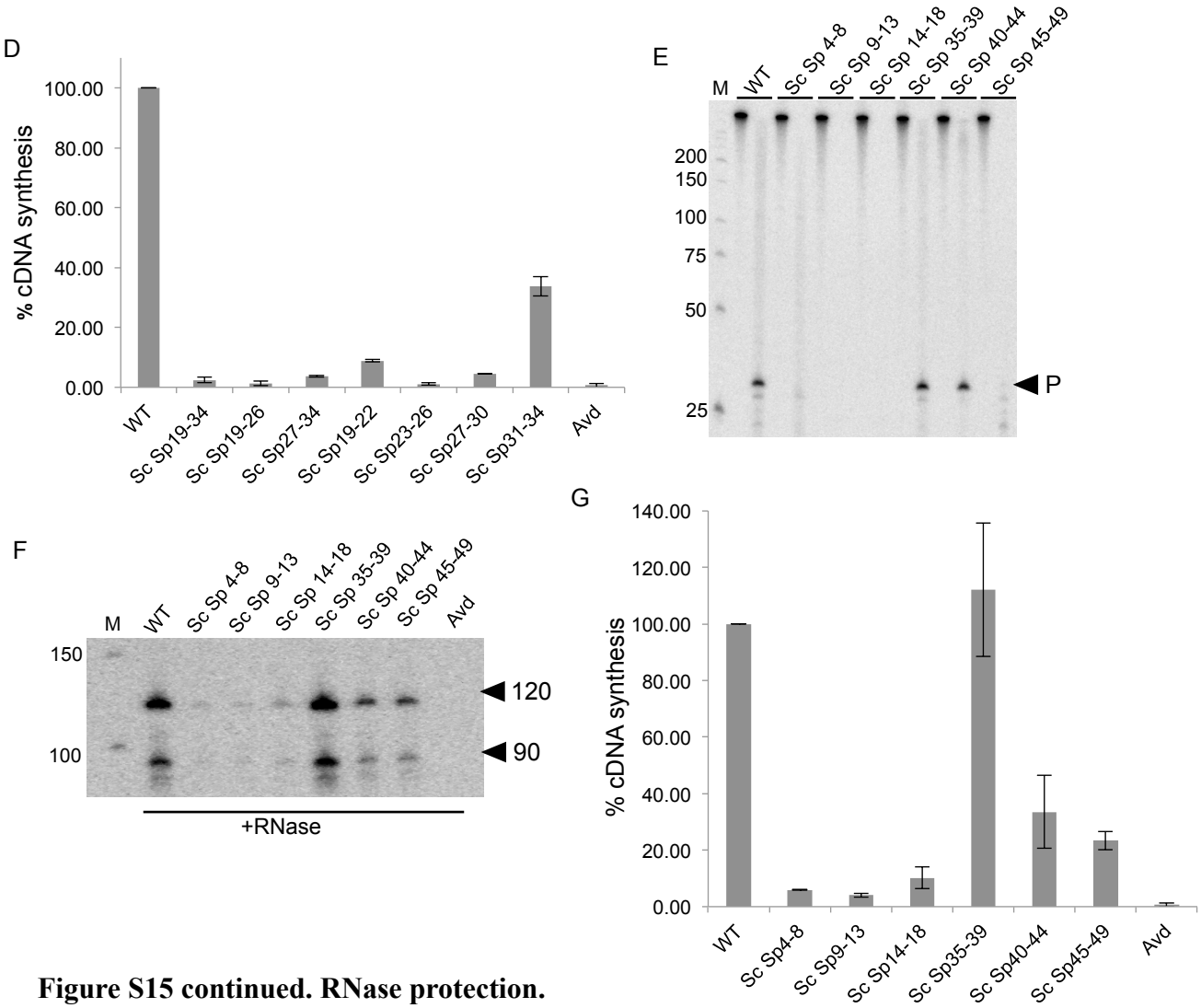

Figure S15 continued. RNase protection.

D. Quantification of gel in Figure 6D. Means and standard deviations from three independent experiments are shown, with values normalized to the WT DGR RNA template.

E. RNase protection by Avd carried out on a internally-labeled 580 nt DGR template, either wild-type or with scrambled (Sc) Sp sequences. The first lane in each pair was untreated and the second RNase-treated, and resolved by denaturing PAGE. The position of the protected (P) band is indicated.

F. Radiolabeled products resulting from bRT-Avd activity with 580 nt DGR RNA, either wild-type or containing scrambled (Sc) sequences, as template. The last lane shows the activity of Avd alone with wild-type 580 nt DGR RNA as template. Products were treated with RNase, and resolved by denaturing PAGE. The positions of the 120 and 90 nt cDNAs are indicated.

G. Quantification of cDNA synthesis by bRT-Avd from the 580 nt DGR RNA, either wild-type or containing scrambled (Sc) Sp sequences. The "Avd" sample shows the activity of Avd alone with wild-type 580 nt DGR RNA as template. Means and standard deviations from three independent experiments shown, with values normalized to bRT-Avd activity with the wild-type 580 nt DGR RNA template.